



Comprehensive Test Report

Regression Tests • Benchmarks • Physics Diagnostics

Generated: 2026-03-10 16:03:09

VegasAfterglow 2.0.2.dev79 | Python 3.12.9

Commit: c33f3812 | Platform: Darwin arm64

CPU: Apple M2

Powered by Claude Code

Table of Contents

1. Regression Tests

How to Read

1.1 Dynamics

Dynamics Summary

Forward Shock (ISM)

Forward Shock (Wind)

Reverse Shock Thin (ISM)

Reverse Shock Thin (Wind)

Reverse Shock Thick (ISM)

Reverse Shock Thick (Wind)

1.2 Radiation

1.2.1 Synchrotron Spectrum Shapes

Spectrum Summary

Spectrum Detail

1.2.2 Characteristic Frequencies

Frequencies Summary

Forward Shock (ISM)

Forward Shock (Wind)

Reverse Shock Thin (ISM)

Reverse Shock Thin (Wind)

Reverse Shock Thick (ISM)

Reverse Shock Thick (Wind)

2. Benchmark Results

How to Read

On-axis Overview

Off-axis Overview

Convergence Summary

Error Distribution

Section 1

Regression Tests

Power-law scaling verification against theoretical predictions

Regression Test Report Guide

This document describes the regression validation framework for VegasAfterglow, which verifies that simulation outputs reproduce the expected power-law scaling relations from GRB afterglow theory.

1. Test Categories

The regression suite validates physical quantities against analytical predictions derived from standard synchrotron afterglow theory. Tests cover both forward and reverse shocks:

Forward shock:

1. **Shock dynamics:** Lorentz factor, radius, magnetic field, particle number 2. **Characteristic frequencies:** ν_m (injection), ν_c (cooling), ν_M (maximum) 3. **Spectral shapes:** Power-law indices in different frequency regimes

Reverse shock:

4. **Thin-shell dynamics:** Shock dynamics during and after reverse shock crossing (short engine duration) 5. **Thick-shell dynamics:** Shock dynamics during and after reverse shock crossing (long engine duration) 6. **Thin-shell frequencies:** Characteristic frequency evolution during crossing phase 7. **Thick-shell frequencies:** Characteristic frequency evolution during crossing phase

All regression tests use a model resolution of $(0.3, 2, 15)$ to ensure well-resolved evolution for accurate power-law fitting.

2. Evolutionary Phases

2.1 Forward Shock

The blast wave passes through distinct dynamical phases as it decelerates. Each phase exhibits characteristic power-law behavior that serves as a validation target.

Phase	Physics
Coasting	Free expansion, $\Gamma \approx \text{const}$
Blandford-McKee	Self-similar deceleration
Sedov-Taylor	Non-relativistic, $u < 0.1$

2.2 Reverse Shock (Thin Shell)

Short engine duration. The reverse shock crosses the ejecta quickly, then evolves as a decaying blast wave.

Phase	Physics
Crossing	Reverse shock traversing ejecta
Post-crossing	Post-crossing deceleration
Sedov-Taylor	Non-relativistic

2.3 Reverse Shock (Thick Shell)

Long engine duration. The reverse shock crosses while the engine is still active, producing different scaling.

Phase	Physics
Crossing	Reverse shock traversing during engine activity
Post-crossing	Post-crossing deceleration
Sedov-Taylor	Non-relativistic

3. Expected Scaling Relations

3.1 Forward Shock Dynamics

Physical quantities at the shock front scale as power laws with observer time: $Q \propto t^\alpha$. The exponents depend on the external medium density profile.

ISM (constant density n)

Phase	u	r	B	N_p
Coasting	0	1	0	3
Blandford-McKee	-3/8	1/4	-3/8	3/4
Sedov-Taylor	-3/5	2/5	-3/5	6/5

Wind (density $\propto r^{-2}$)

Phase	u	r	B	N_p
Coasting	0	1	-1	1
Blandford-McKee	-1/4	1/2	-3/4	1/2
Sedov-Taylor	-1/3	2/3	-1	2/3

3.2 Forward Characteristic Frequencies

The synchrotron spectrum is characterized by break frequencies that evolve with time: $\nu \propto t^\alpha$.

ISM

Phase	ν_m	ν_c	ν_M
Coasting	0	-2	0
Blandford-McKee	-3/2	-1/2	-3/8
Sedov-Taylor	-3/5	-1/5	0

Wind

Phase	v_m	v_c	v_M
Coasting	-1	-1	0
Blandford-McKee	-3/2	1/2	-1/4
Sedov-Taylor	-1	1	0

3.3 Reverse Shock Dynamics (Thin Shell)

ISM

Phase	u	r	B	N_p
Crossing	3/2	1	0	3/2
Post-crossing	-1/4	1/4	—	0
Sedov-Taylor	-2/5	2/5	—	0

Wind

Phase	u	r	B	N_p
Crossing	1/2	1	-1	1/2
Post-crossing	—	1/2	—	0
Sedov-Taylor	—	2/3	—	0

"—" indicates quantities not tested (insufficiently clean power-law for reliable fitting).

3.4 Reverse Shock Dynamics (Thick Shell)

ISM

Phase	u	r	B	N_p
Crossing	1/4	1/2	-1/4	1
Post-crossing	-1/4	1/4	—	0
Sedov-Taylor	-2/5	2/5	—	0

Wind

Phase	u	r	B	N_p
Crossing	0	1	-1	1
Post-crossing	—	1/2	—	0

Phase	u	r	B	N_p
Sedov-Taylor	—	2/3	—	0

3.5 Reverse Shock Characteristic Frequencies

Frequency scaling is validated during the crossing phase. Post-crossing and Sedov-Taylor frequency tests are not performed for reverse shocks since the reverse shock material is no longer freshly shocked.

Thin Shell — Crossing Phase

Medium	v_m	v_c	v_M
ISM	0	-2	0
Wind	-1	1	0

Thick Shell — Crossing Phase

Medium	v_m	v_c	v_M
ISM	—	-1	-1/4
Wind	-1	1	0

4. Spectral Regimes

The synchrotron spectrum consists of power-law segments joined at break frequencies. The spectral index $\beta = d(\log F_\nu)/d(\log \nu)$ depends on the ordering of ν_a , ν_m , and ν_c .

Regime I: $\nu_a < \nu_m < \nu_c$ (Slow Cooling)

The standard slow-cooling spectrum where electrons cool on timescales longer than the dynamical time.

Frequency Range	β
$\nu < \nu_a$	2
$\nu_a < \nu < \nu_m$	1/3
$\nu_m < \nu < \nu_c$	-(p-1)/2
$\nu > \nu_c$	-p/2

Regime II: $\nu_m < \nu_a < \nu_c$

Self-absorption frequency lies between the injection and cooling frequencies.

Frequency Range	β
$\nu < \nu_m$	2

Frequency Range	β
$\nu_m < \nu < \nu_a$	5/2
$\nu_a < \nu < \nu_c$	-(p-1)/2
$\nu > \nu_c$	-p/2

Regime III: $\nu_a < \nu_c < \nu_m$ (Fast Cooling)

Fast-cooling regime where electrons radiate most of their energy before the next dynamical time.

Frequency Range	β
$\nu < \nu_a$	2
$\nu_a < \nu < \nu_c$	1/3
$\nu_c < \nu < \nu_m$	-1/2
$\nu > \nu_m$	-p/2

Regime IV: $\nu_c < \nu_a < \nu_m$

Self-absorption occurs above the cooling frequency in fast-cooling conditions.

Frequency Range	β
$\nu < \nu_c$	2
$\nu_c < \nu < \nu_a$	2
$\nu_a < \nu < \nu_m$	-1/2
$\nu > \nu_m$	-p/2

Regime V: $\nu_c < \nu_m < \nu_a$

Heavily self-absorbed fast-cooling spectrum.

Frequency Range	β
$\nu < \nu_c$	2
$\nu_c < \nu < \nu_m$	2
$\nu_m < \nu < \nu_a$	5/2
$\nu > \nu_a$	-p/2

The electron index $p = 2.2$ is used, giving $-(p-1)/2 = -0.6$ and $-p/2 = -1.1$.

5. Summary Grid Interpretation

The summary page provides a compact view of all regression tests, allowing rapid identification of any deviations from expected behavior.

Grid Layout

- Rows: Physical quantities (u , r , B , N_p for shock; v_m , v_c , v_M for frequencies; regimes I-V for spectra)
- Columns: Medium (ISM/Wind) subdivided by phase (Coasting, Blandford-McKee, Sedov-Taylor)

Cell Contents

Each cell displays the comparison between simulation and theory:

- Top value: Measured power-law exponent
- Bottom value: Expected theoretical value

Color Coding

Color	Status	Criterion		
Green	Pass		measured - expected	< tolerance
Red	Fail		measured - expected	>= tolerance
Gray	N/A	Insufficient data or not applicable		

Tolerances

- Shock dynamics: 0.1
 - Characteristic frequencies: 0.1
 - Spectral shapes: 0.15
-

6. Detailed Plot Interpretation

The detailed plots provide diagnostic information for understanding any discrepancies identified in the summary grid.

Forward Shock Dynamics Plots (2x2 grid per medium)

Each panel shows two subplots:

- Upper: Quantity vs time (log-log), with phase regions color-coded
- Lower: Local power-law exponent $d(\log Q)/d(\log t)$

Dashed lines indicate expected scaling. Markers show fitted values. Agreement between markers and dashed lines confirms correct implementation.

Reverse Shock Dynamics Plots

Same layout as forward shock, with separate pages for thin-shell and thick-shell configurations. The crossing phase is highlighted distinctly from the post-crossing and deep Newtonian phases.

Characteristic Frequency Plots

Same layout as shock dynamics, tracking v_m , v_c , and v_M evolution. The frequency ordering determines which spectral regime applies at each time.

Spectrum Shape Plots (per regime)

Each regime has a dedicated plot showing:

- Upper: F_ν vs ν with break frequencies marked as vertical lines
- Lower: Spectral index $\beta = d(\log F_\nu)/d(\log \nu)$

Colored regions indicate frequency segments between breaks. Flat regions in the lower panel confirm correct power-law behavior within each segment.

Dynamics Summary: 60/60 passed (100%)

Forward Shock (24/24)



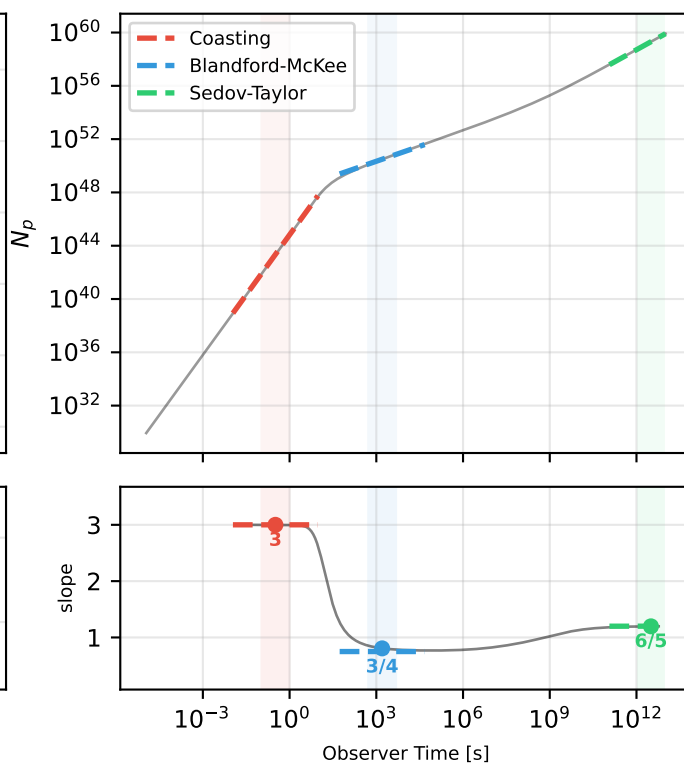
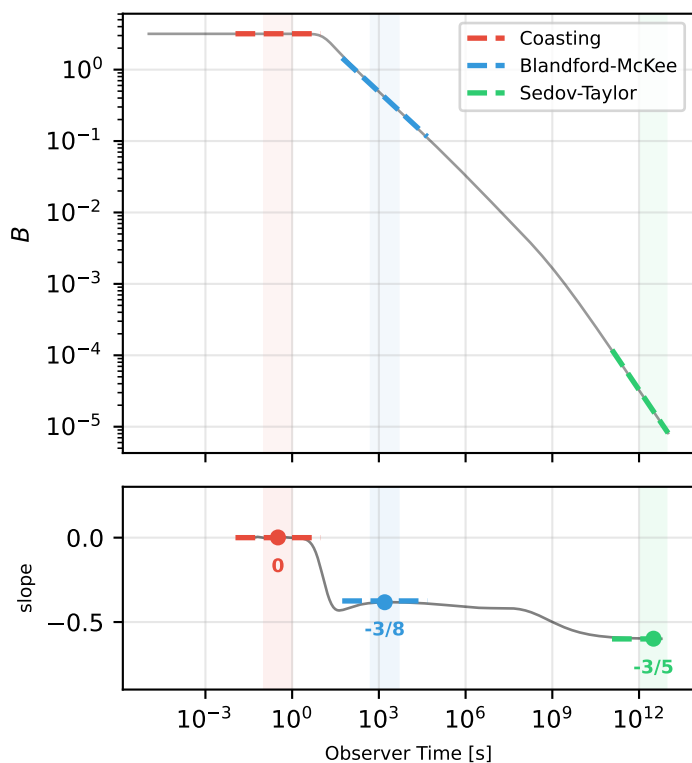
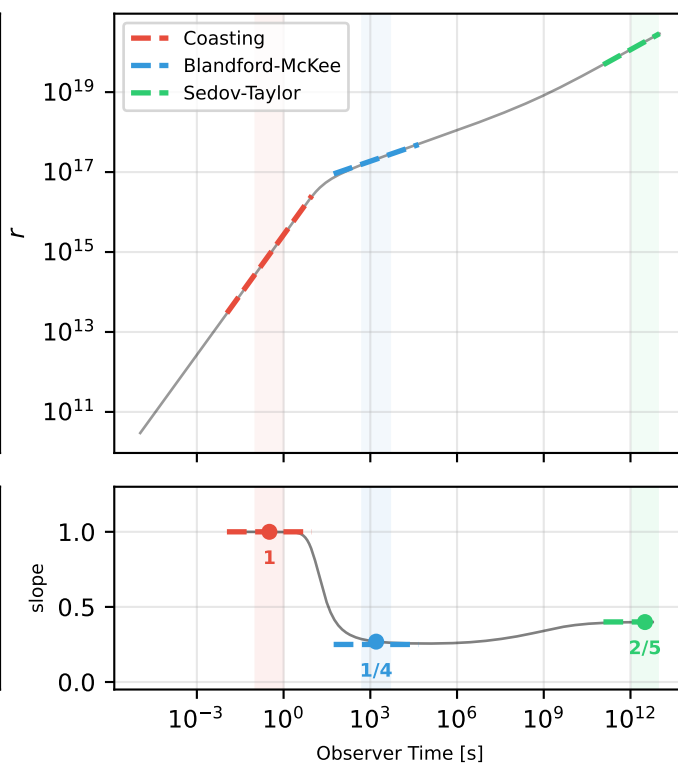
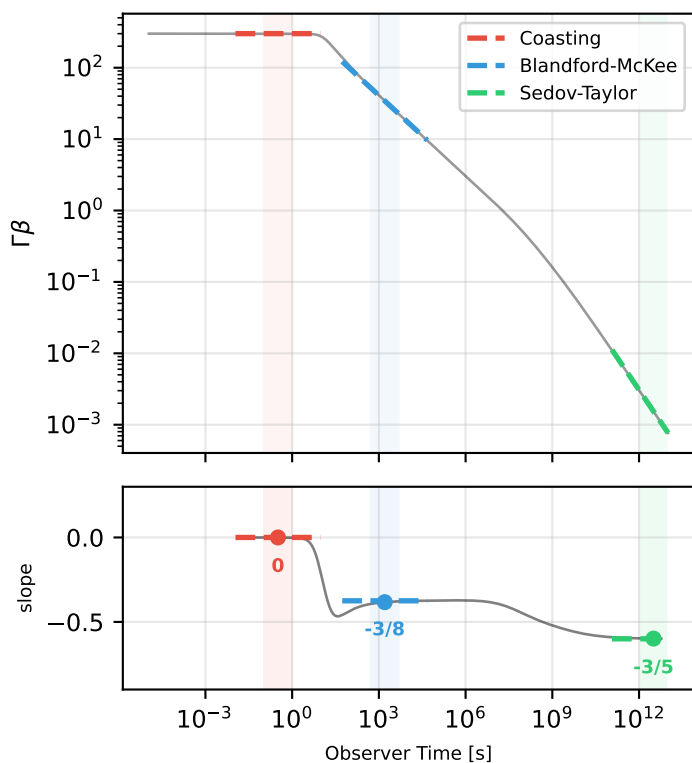
Reverse Shock — Thin Shell (18/18)



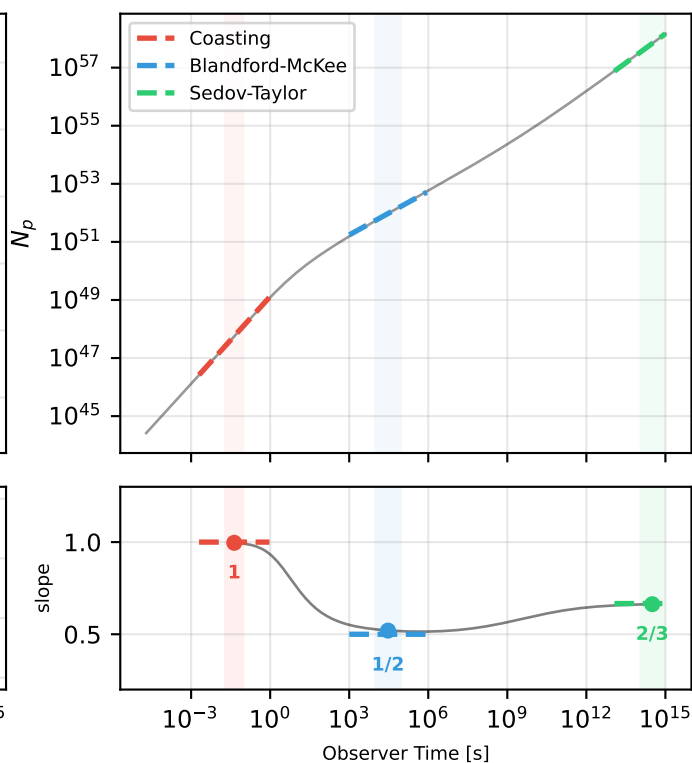
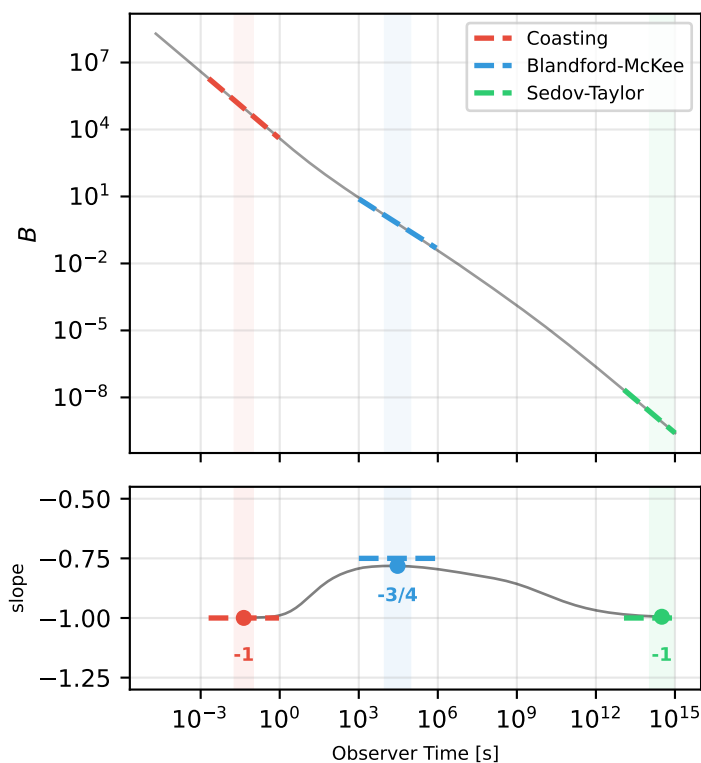
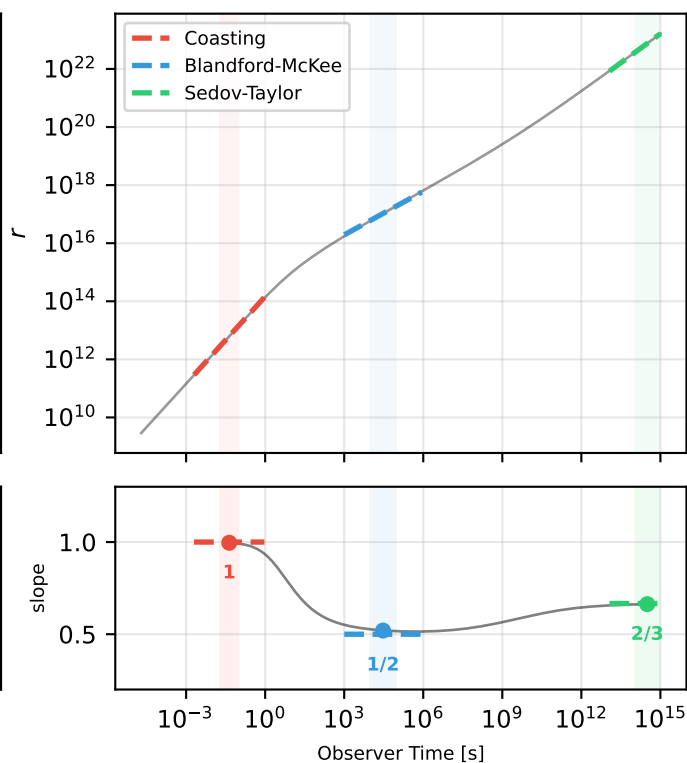
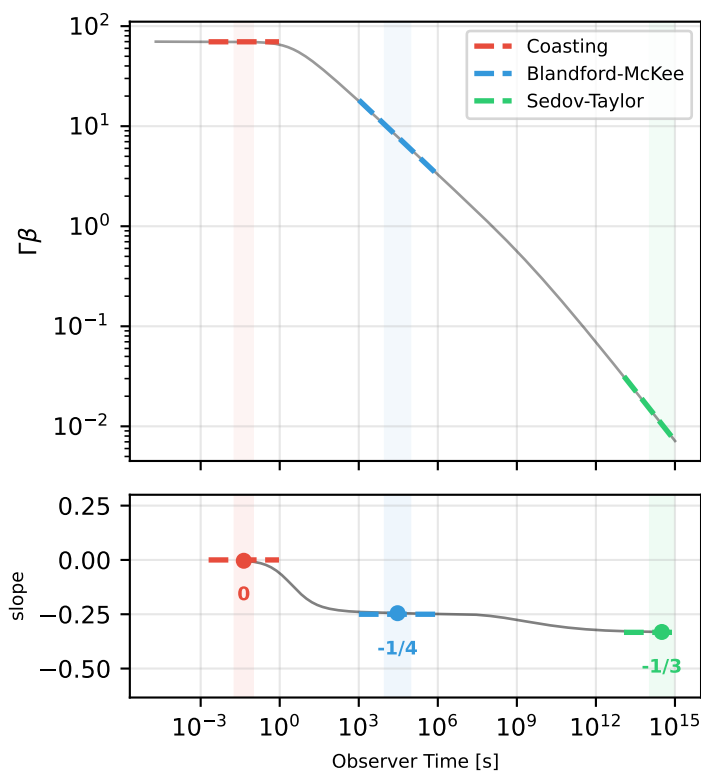
Reverse Shock — Thick Shell (18/18)



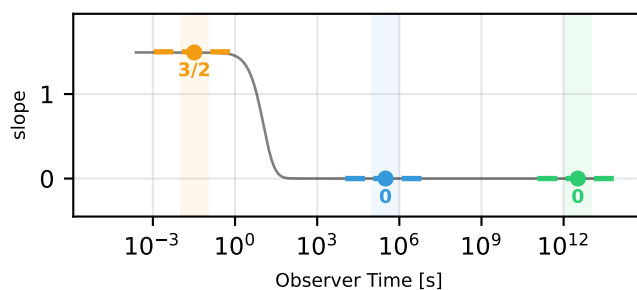
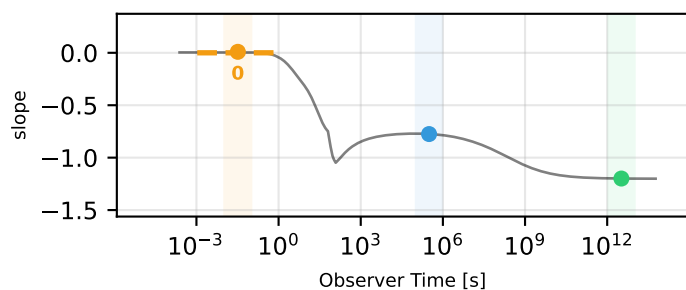
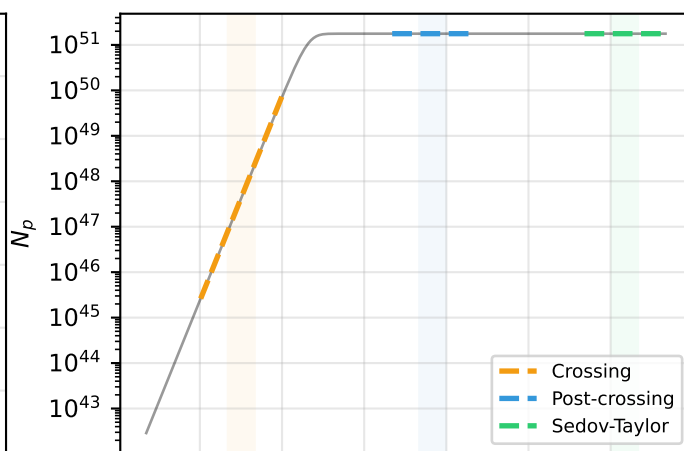
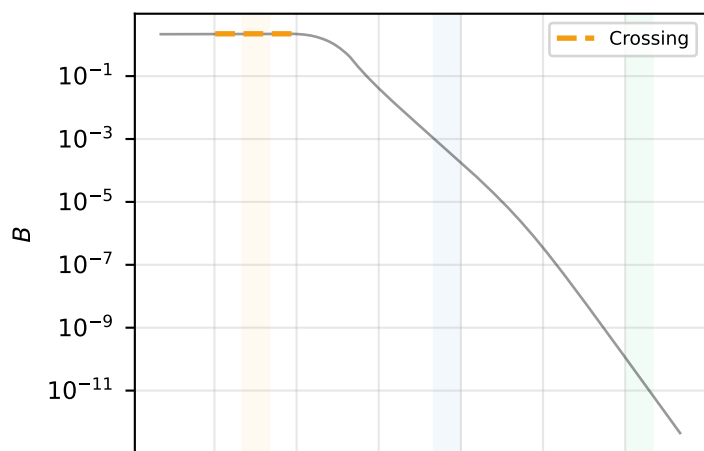
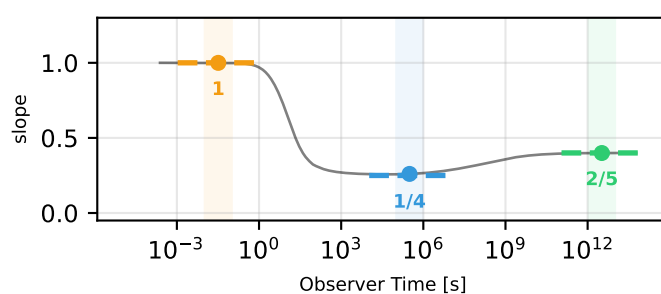
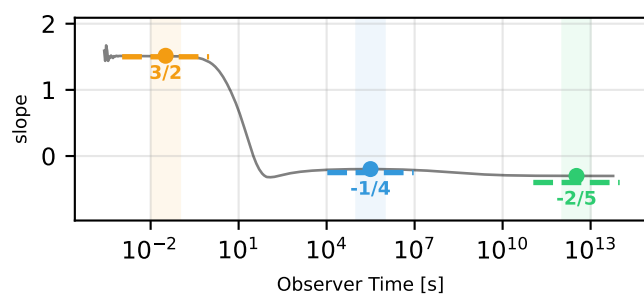
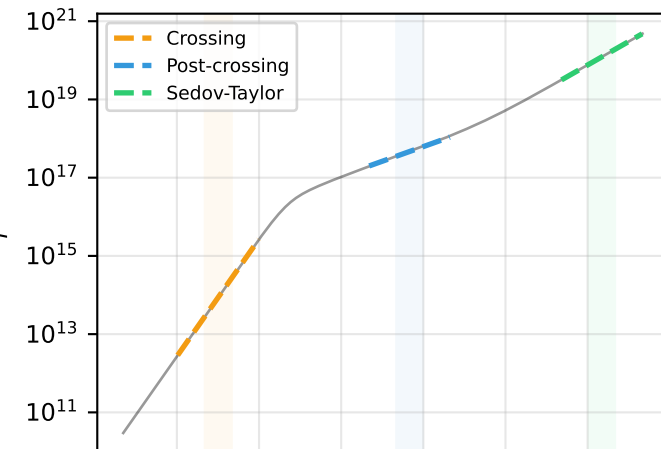
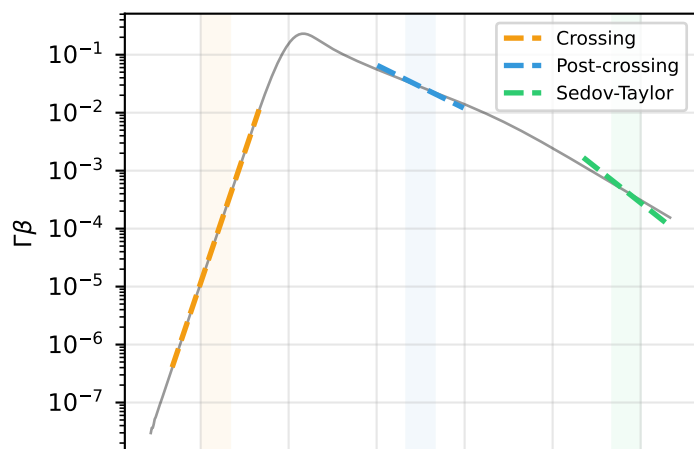
Forward Shock Dynamics: ISM



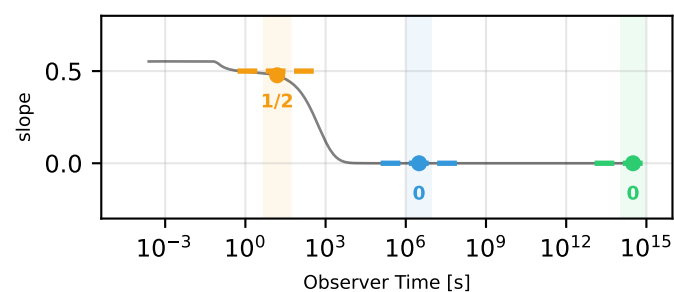
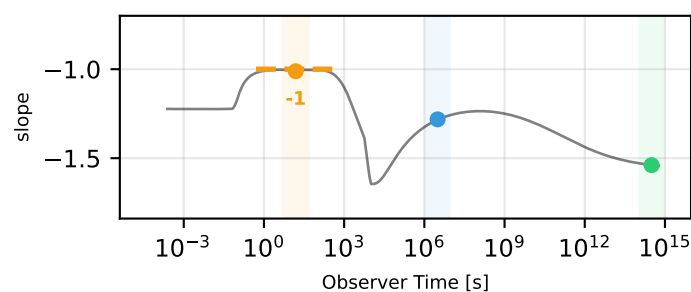
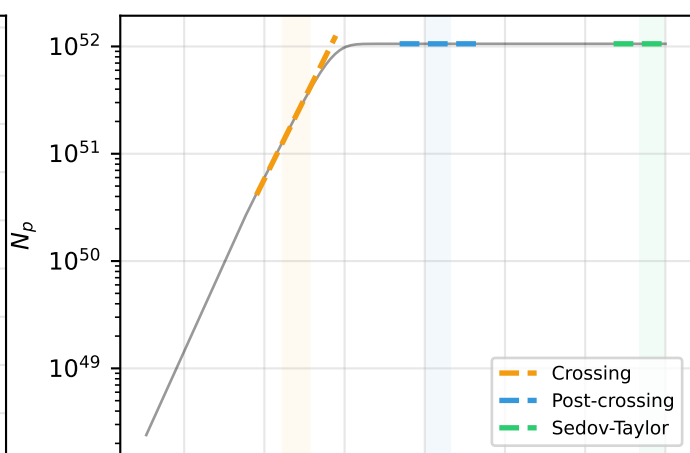
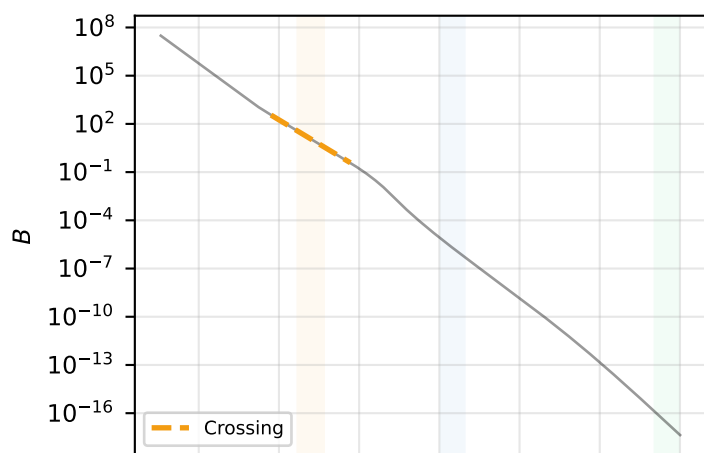
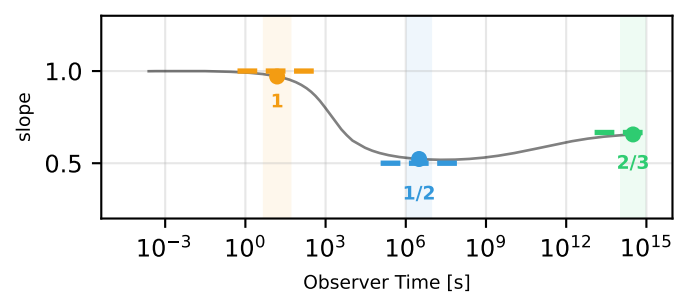
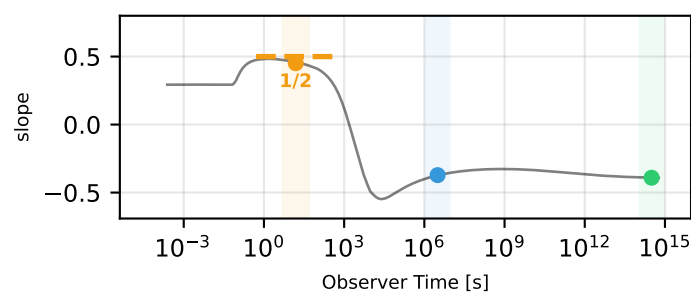
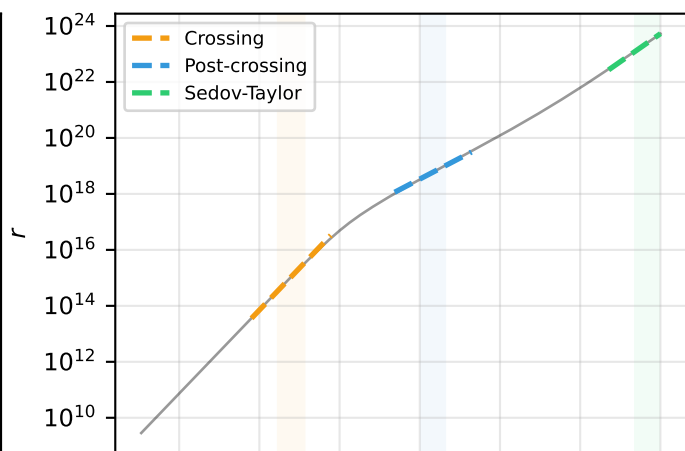
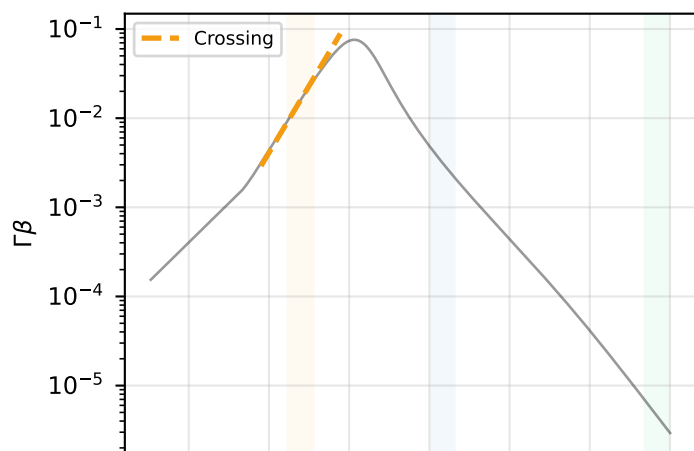
Forward Shock Dynamics: Wind



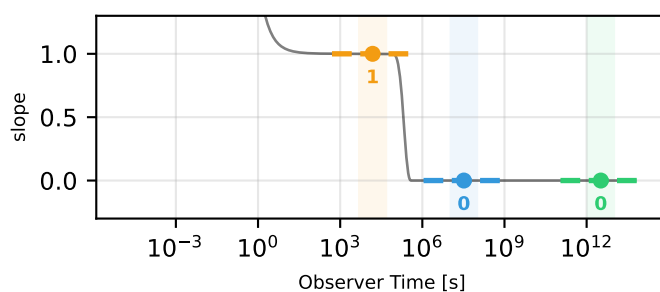
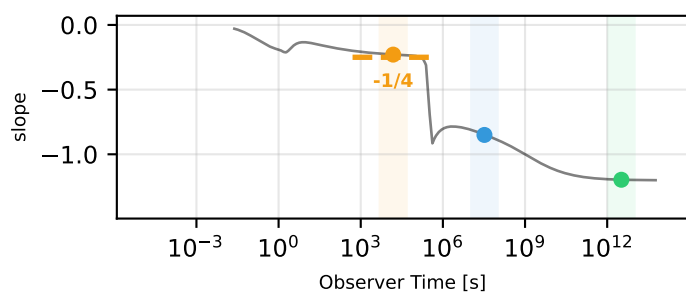
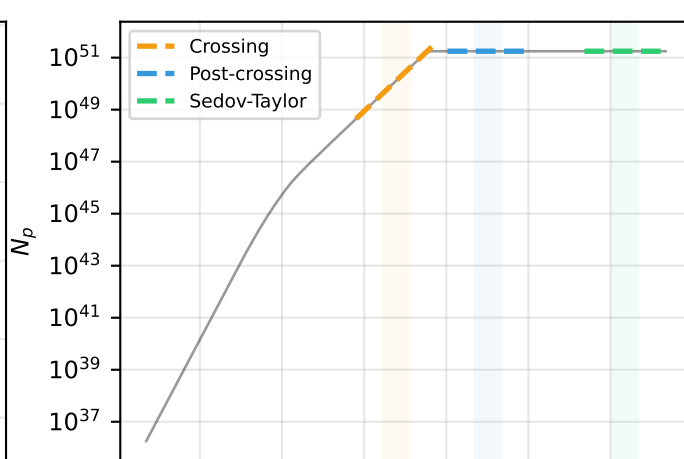
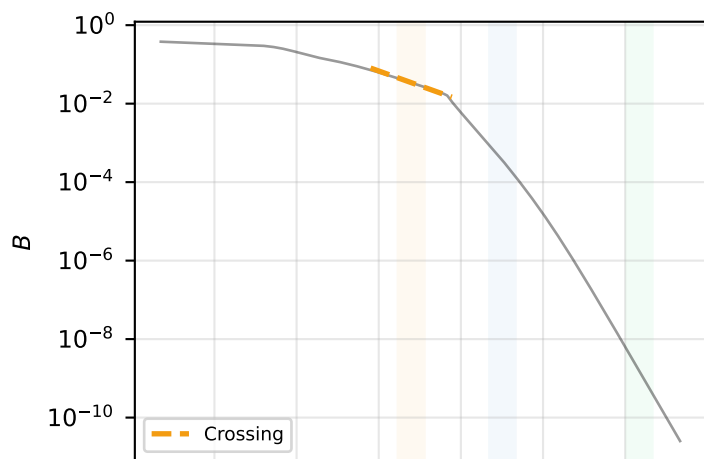
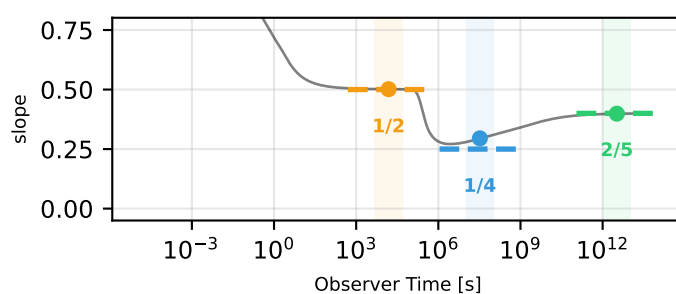
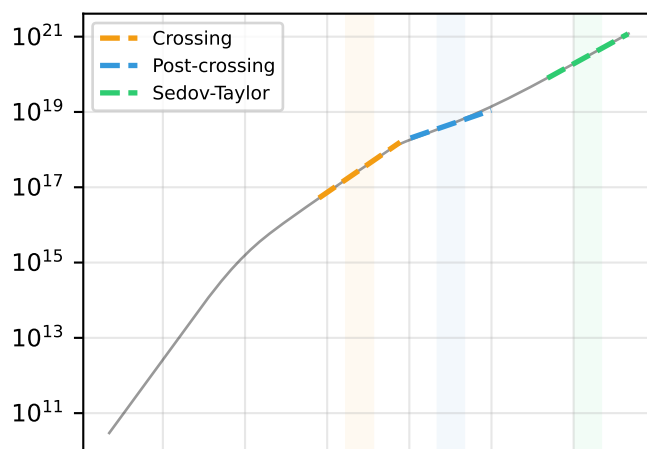
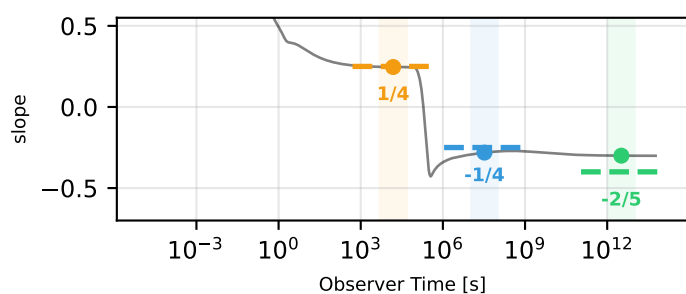
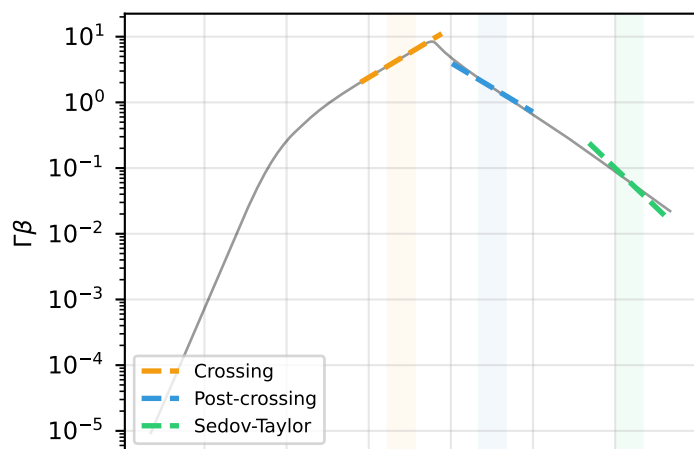
Reverse Shock Dynamics — Thin Shell: ISM



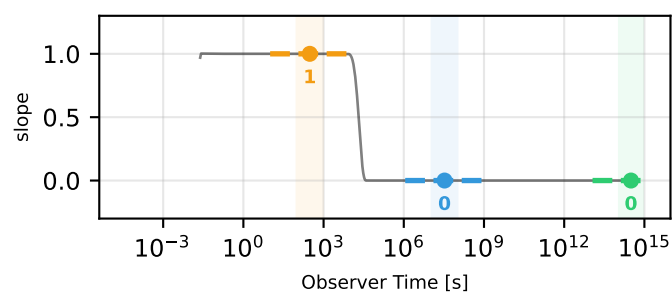
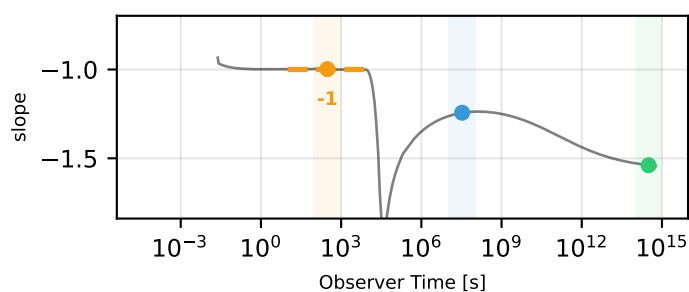
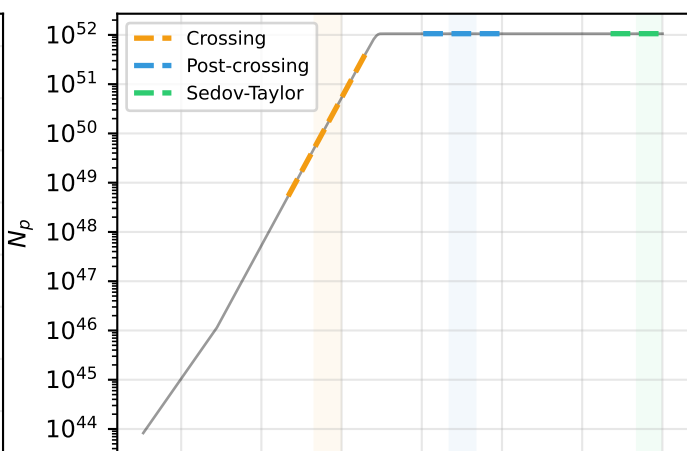
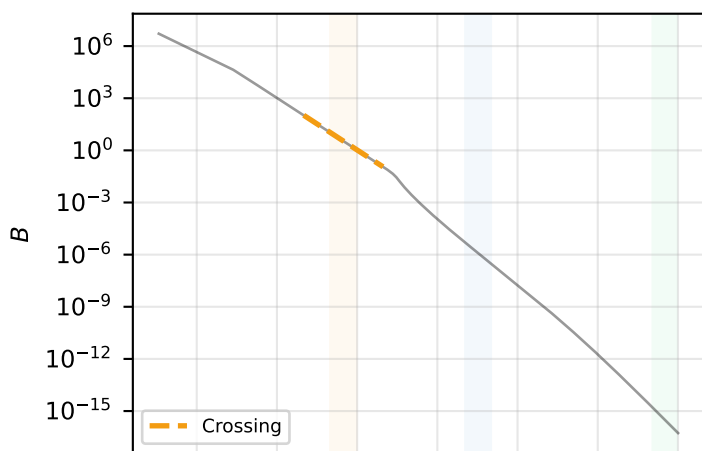
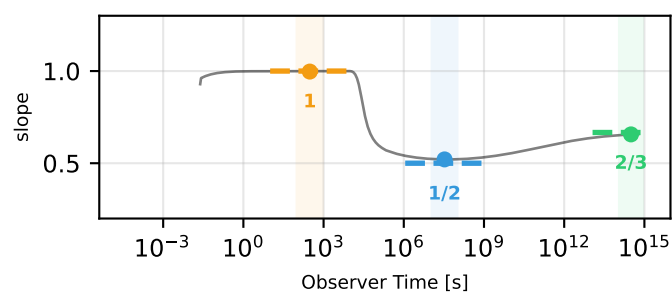
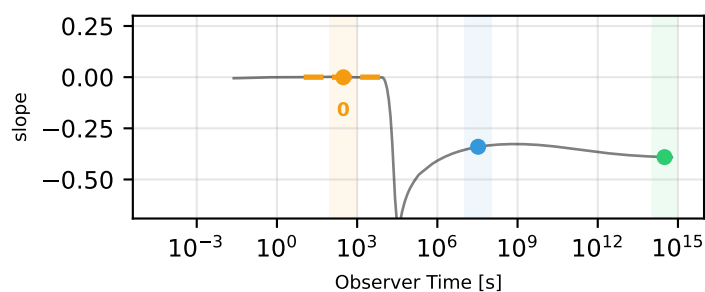
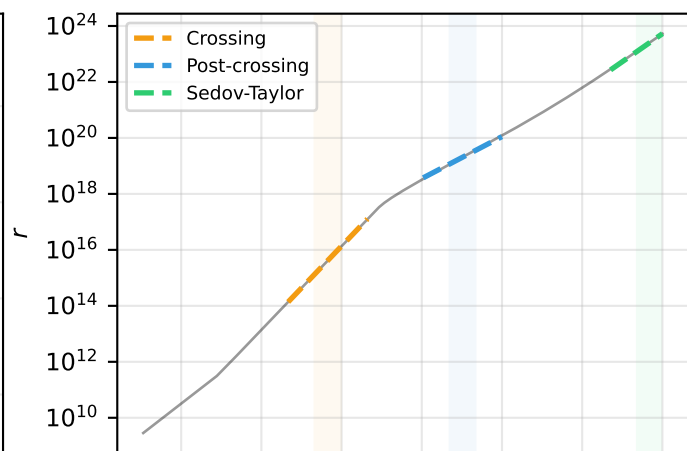
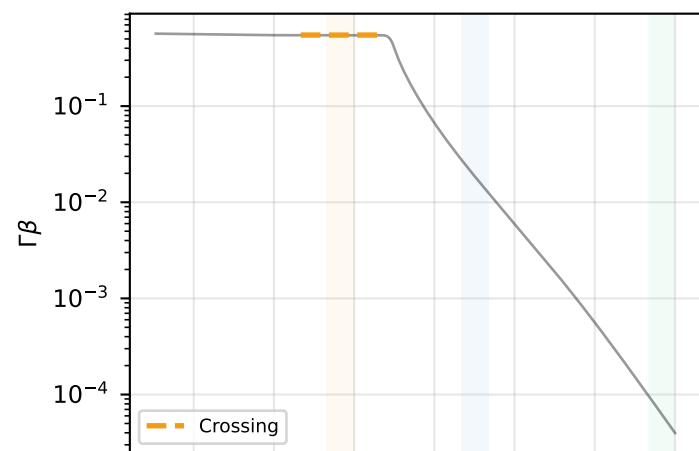
Reverse Shock Dynamics — Thin Shell: Wind



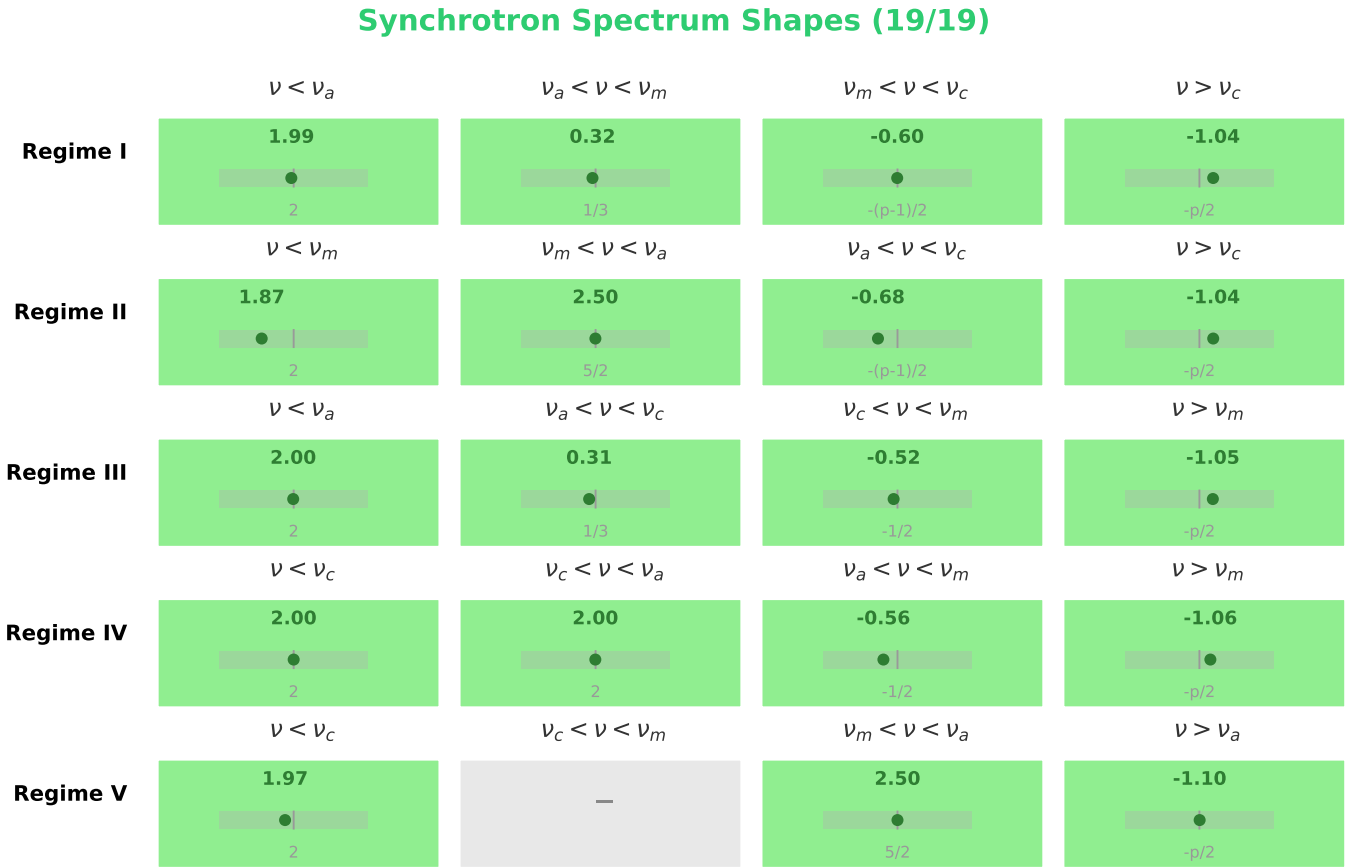
Reverse Shock Dynamics — Thick Shell: ISM



Reverse Shock Dynamics — Thick Shell: Wind

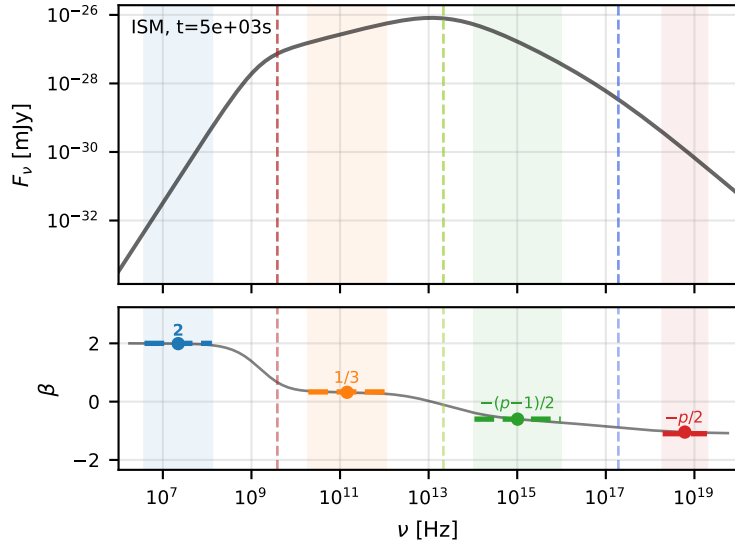


Synchrotron Spectrum Shapes: 19/19 passed (100%)

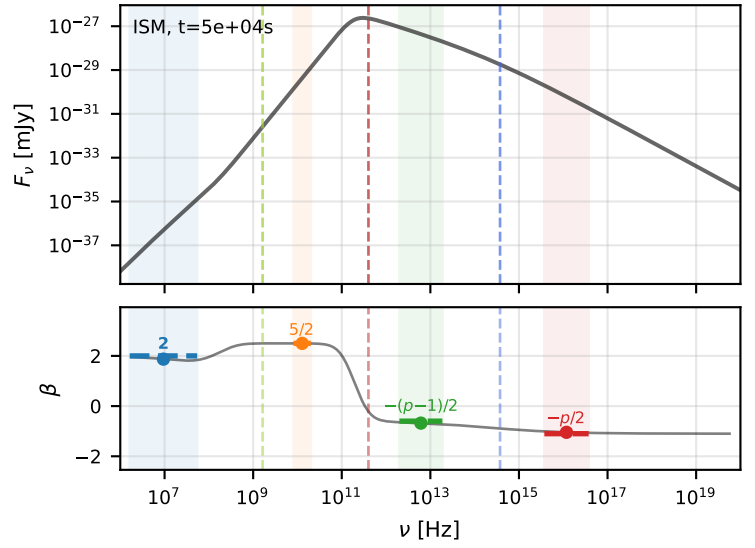


Synchrotron Spectrum Shapes: Spectral Index Verification

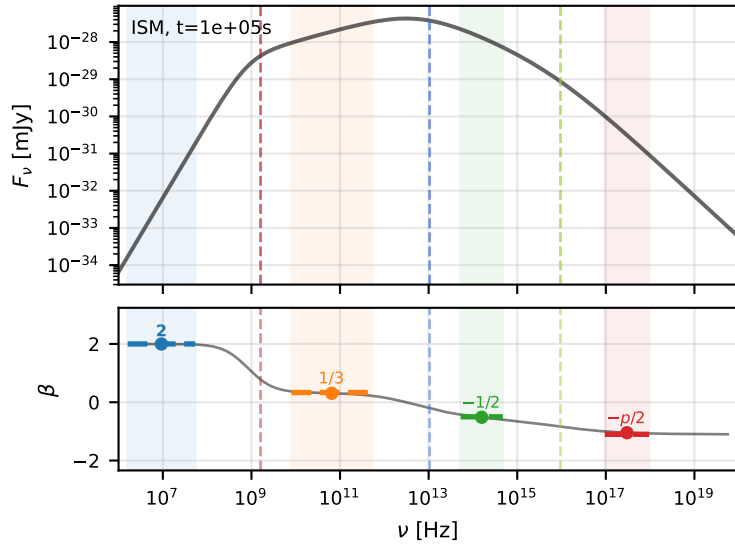
Regime I: $\nu_a < \nu_m < \nu_c$



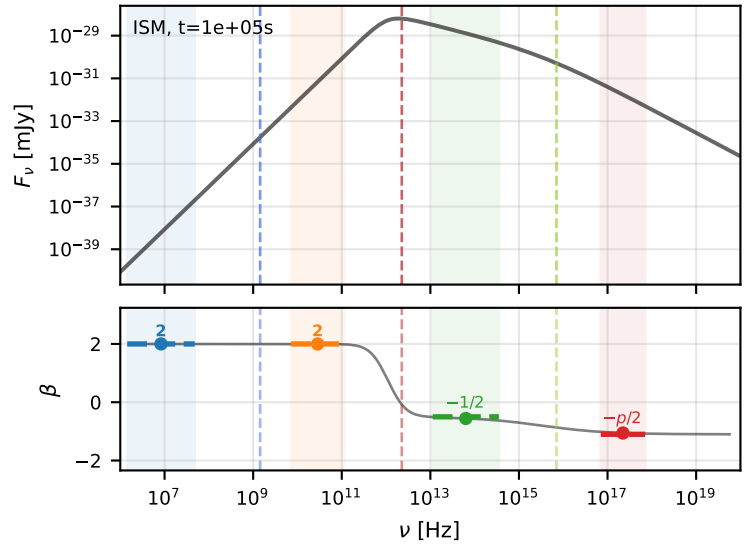
Regime II: $\nu_m < \nu_a < \nu_c$



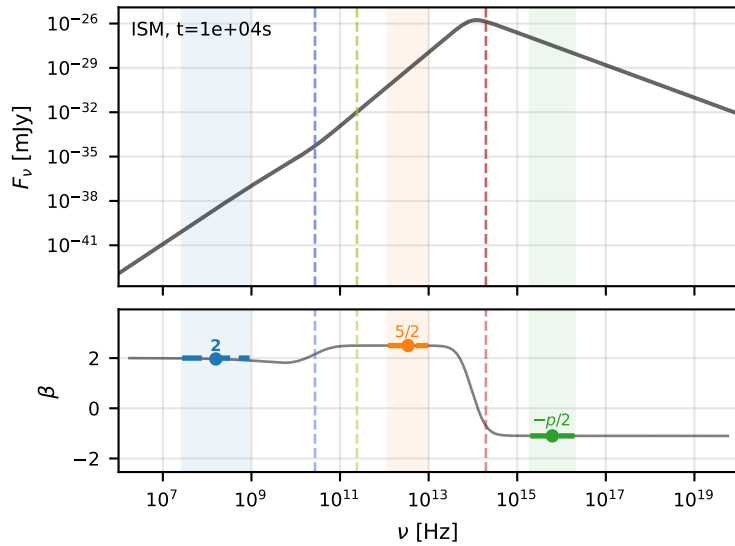
Regime III: $\nu_a < \nu_c < \nu_m$



Regime IV: $\nu_c < \nu_a < \nu_m$

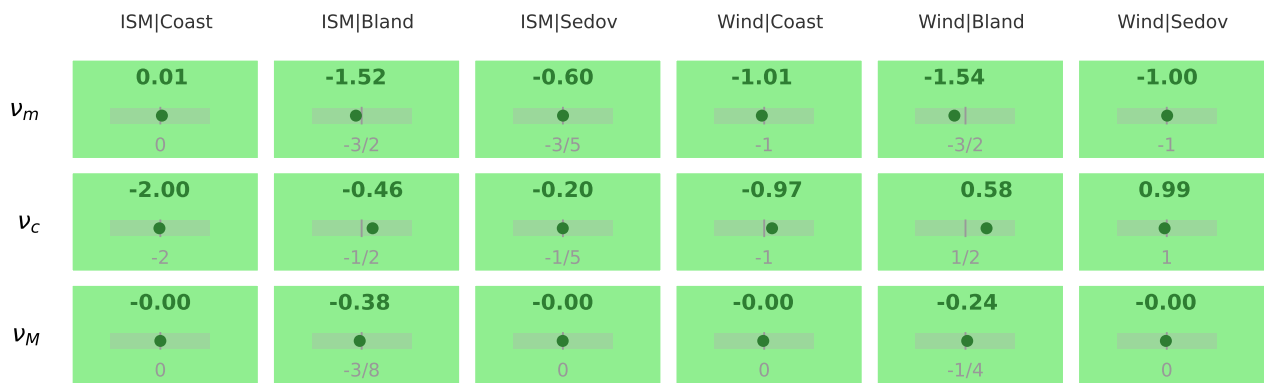


Regime V: $\nu_c < \nu_m < \nu_a$

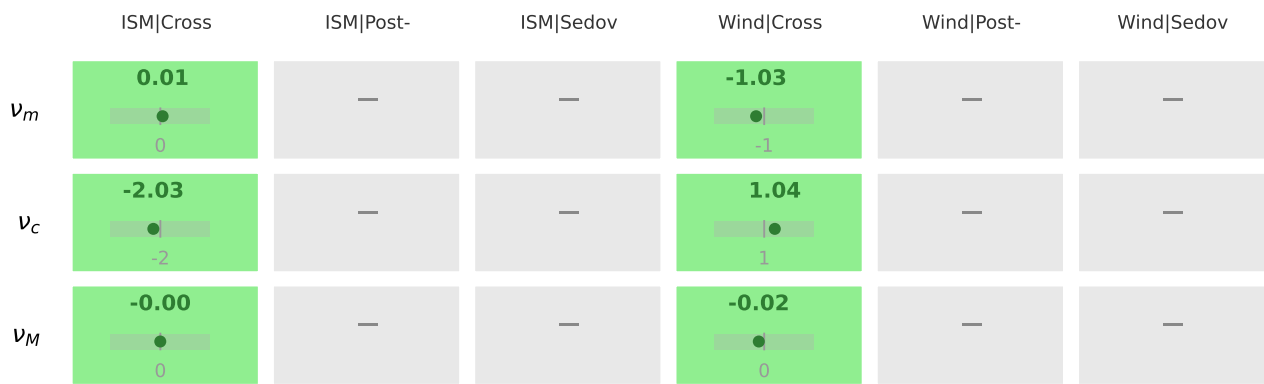


Frequencies Summary: 29/29 passed (100%)

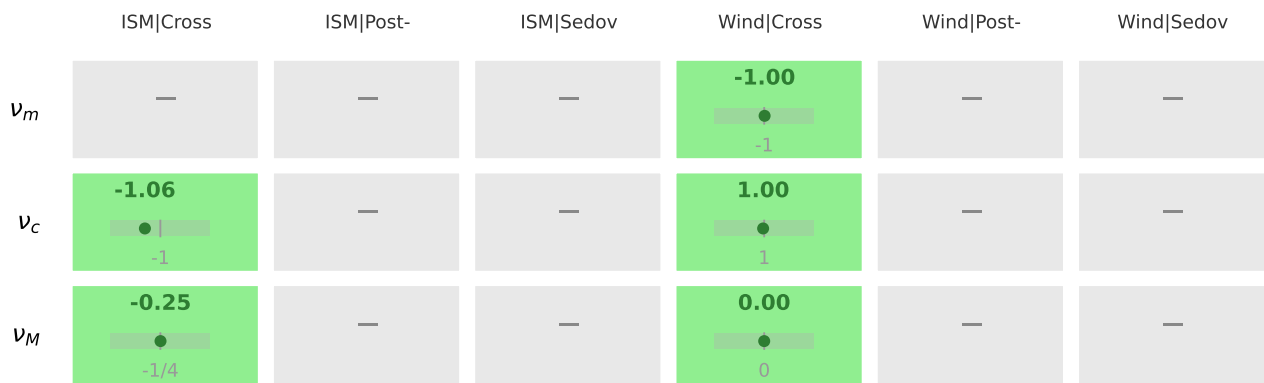
Forward Shock (18/18)



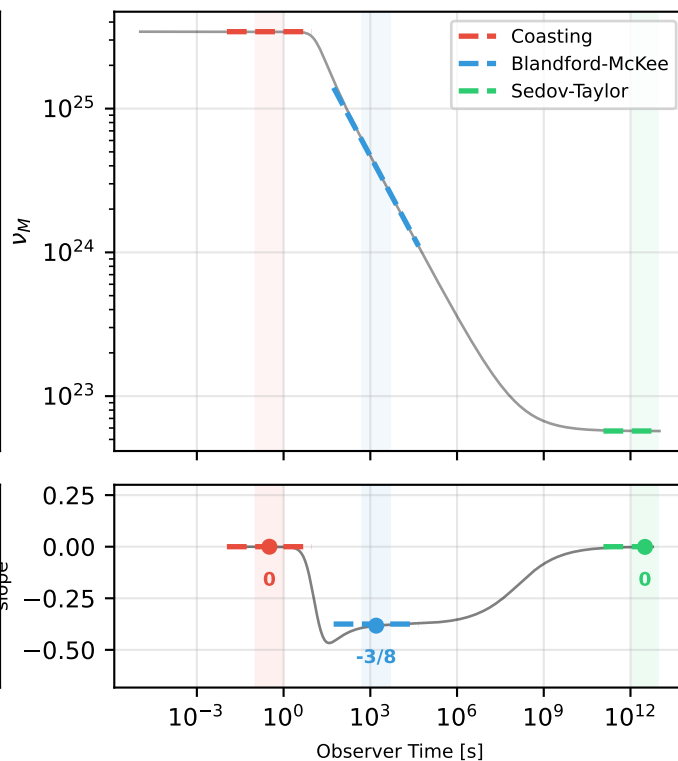
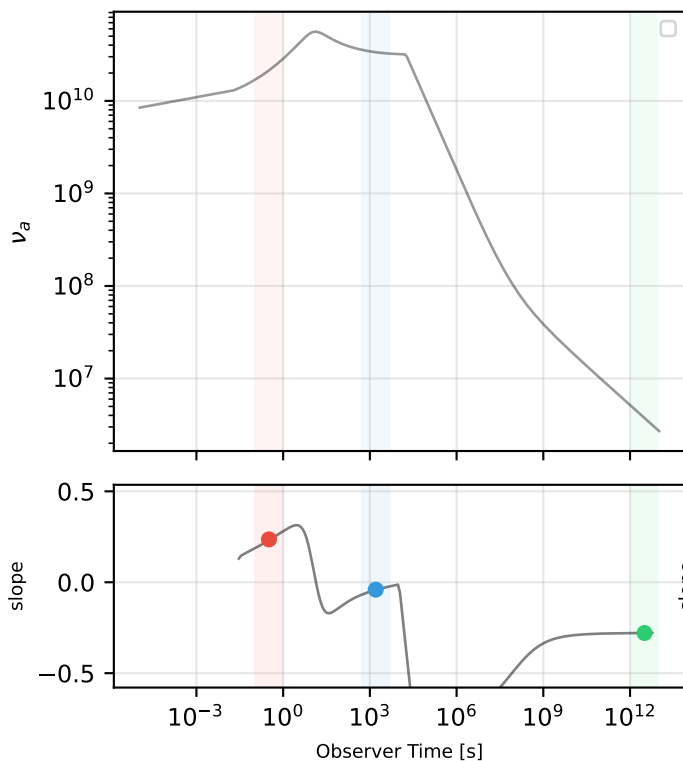
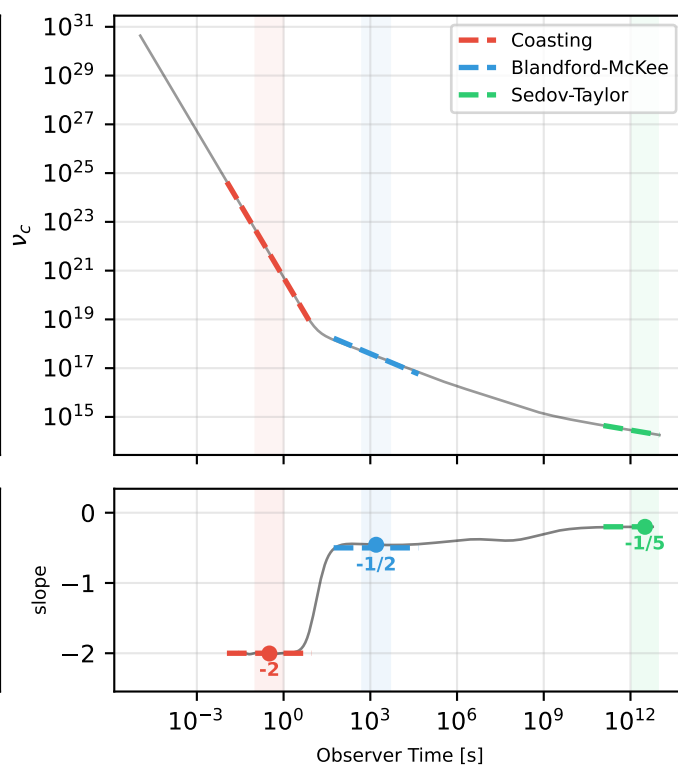
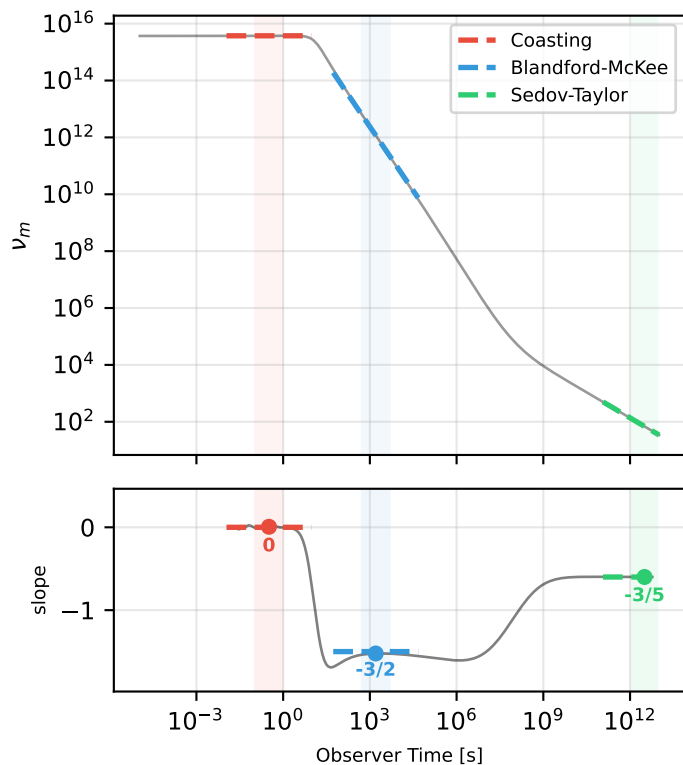
Reverse Shock — Thin Shell (6/6)



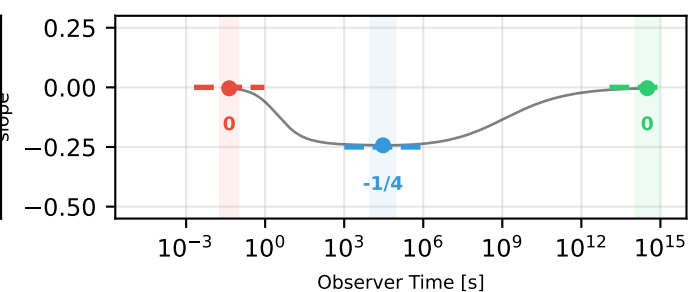
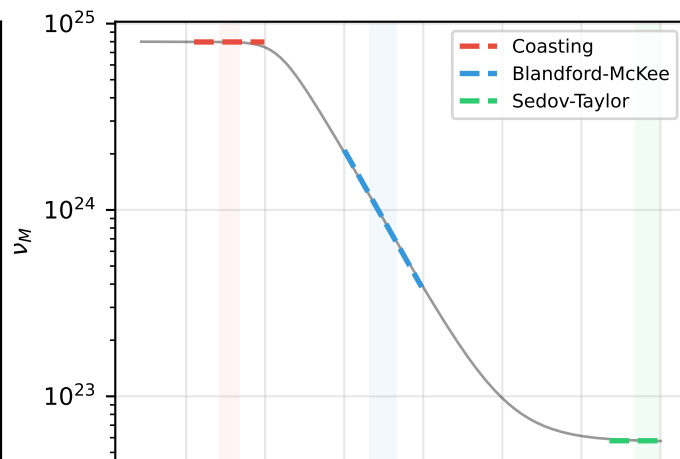
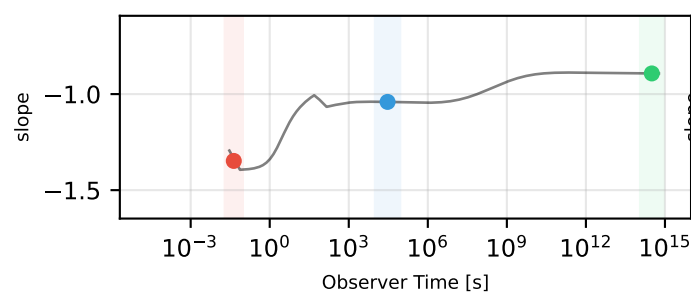
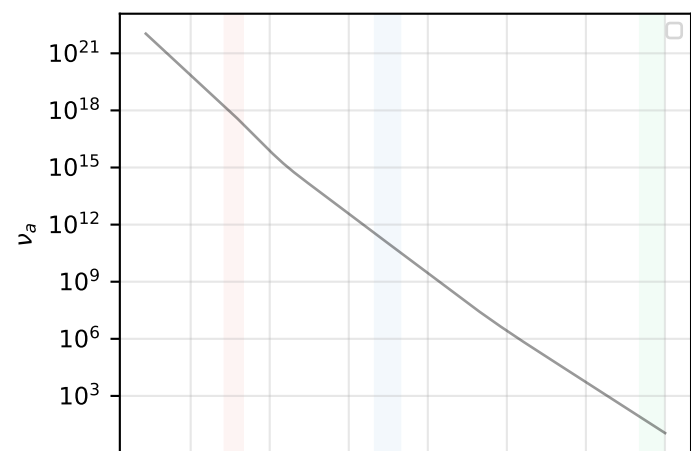
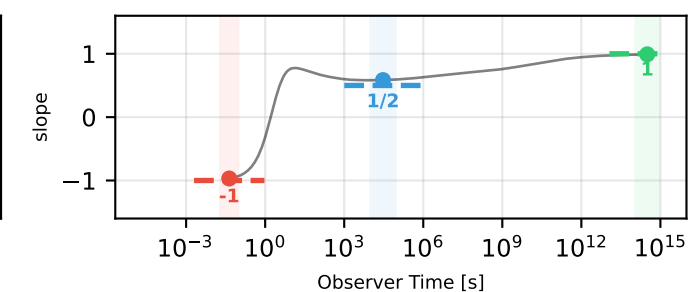
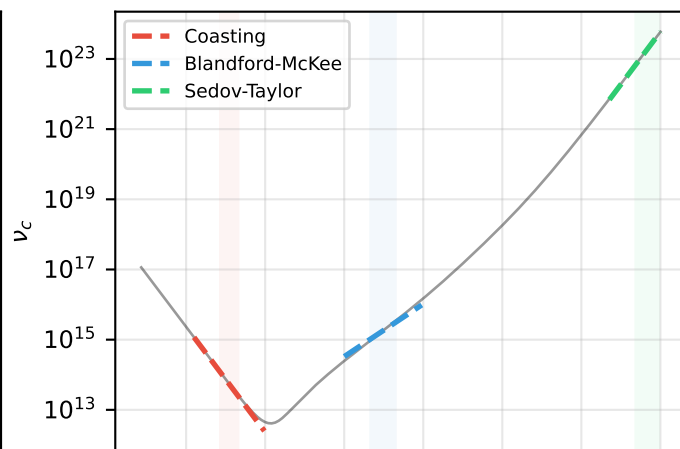
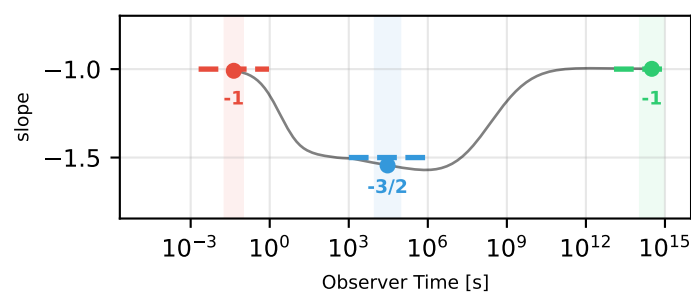
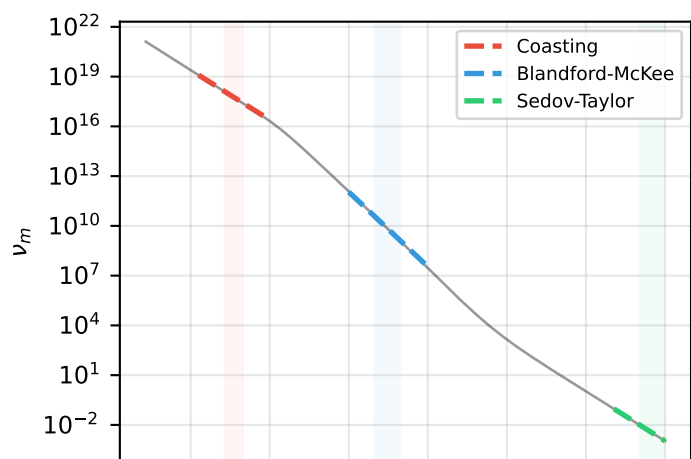
Reverse Shock — Thick Shell (5/5)



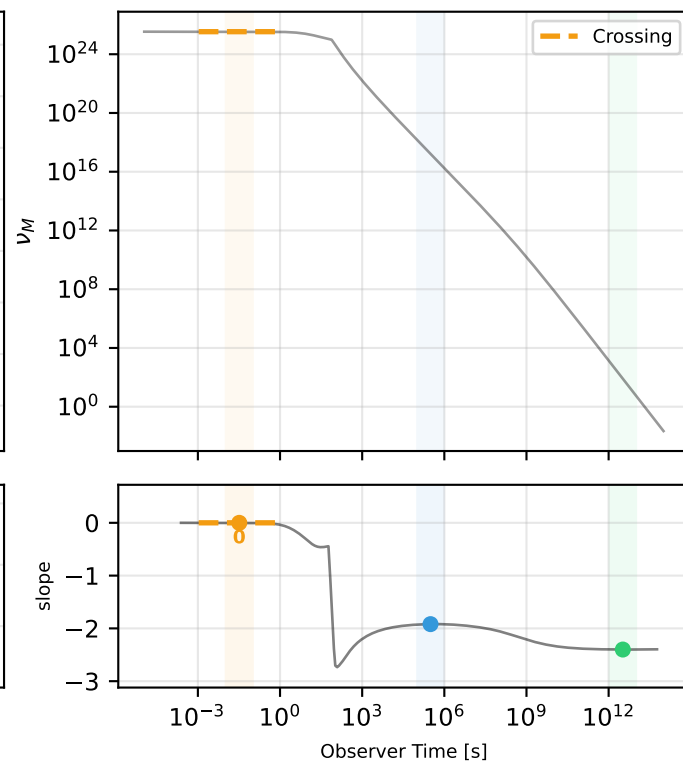
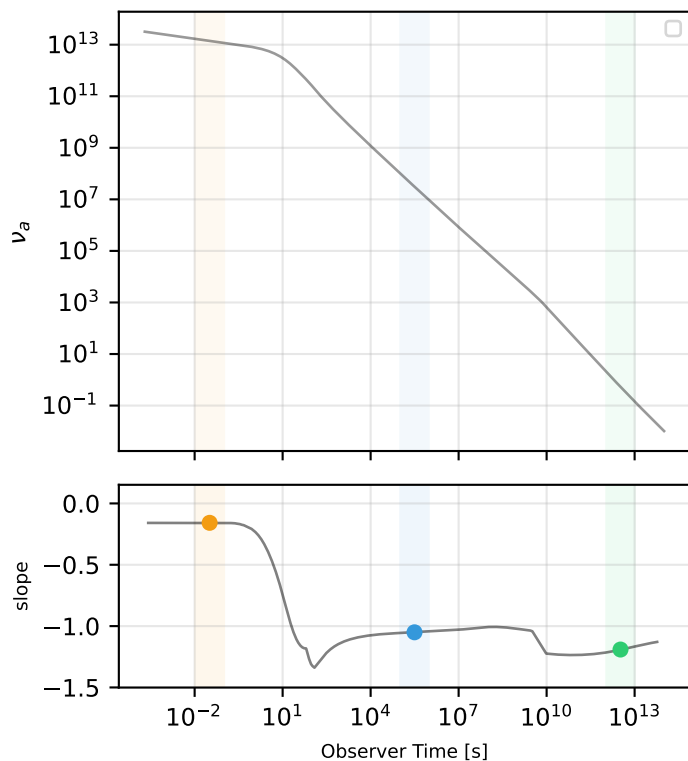
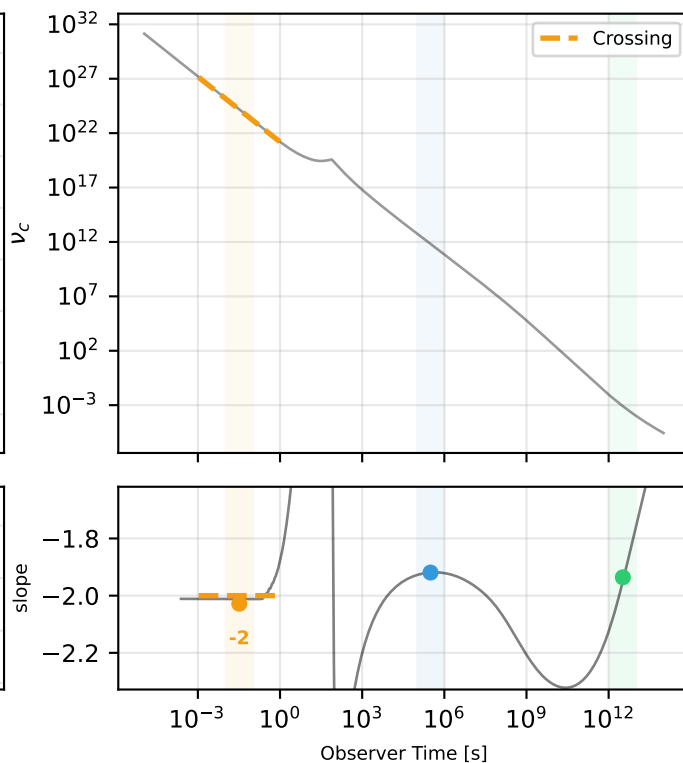
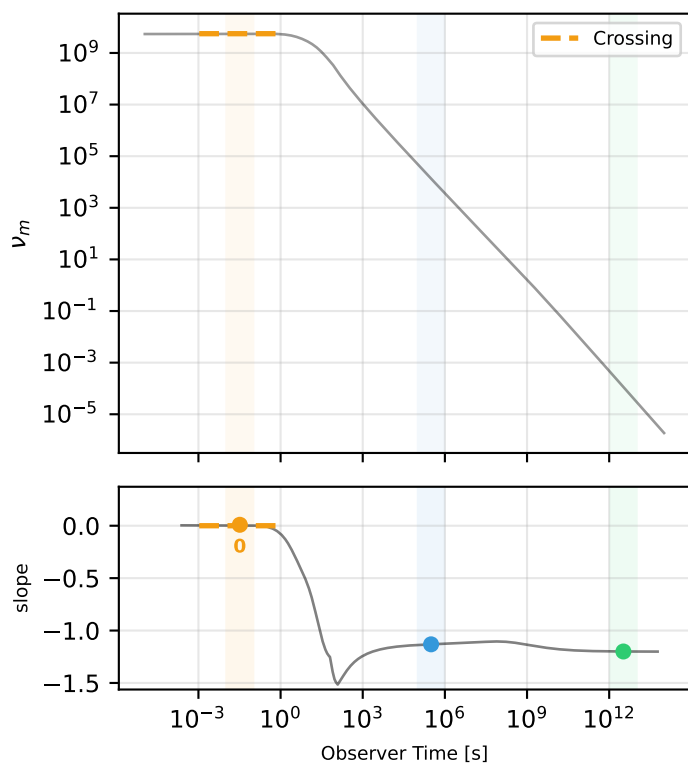
Forward Shock Frequencies: ISM



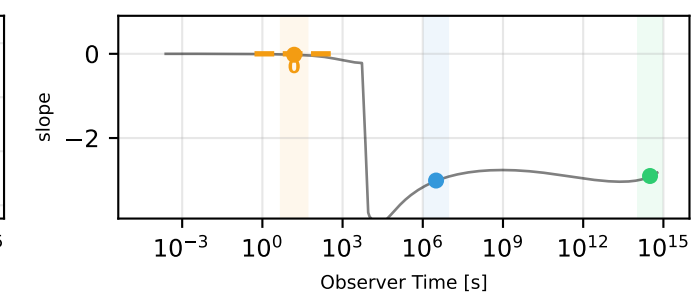
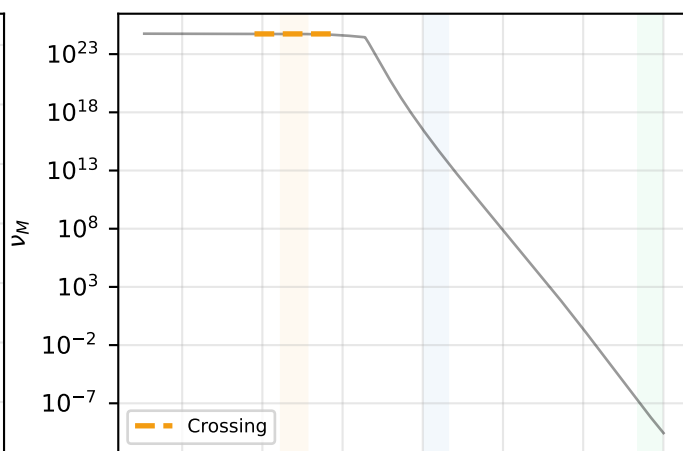
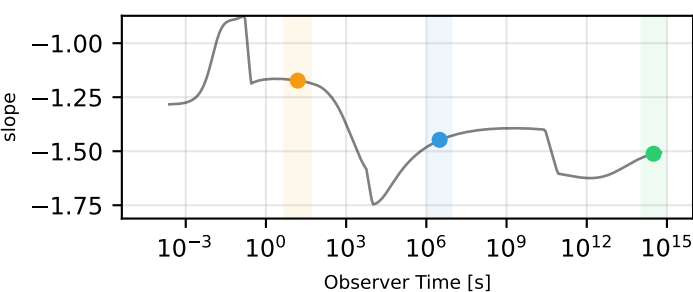
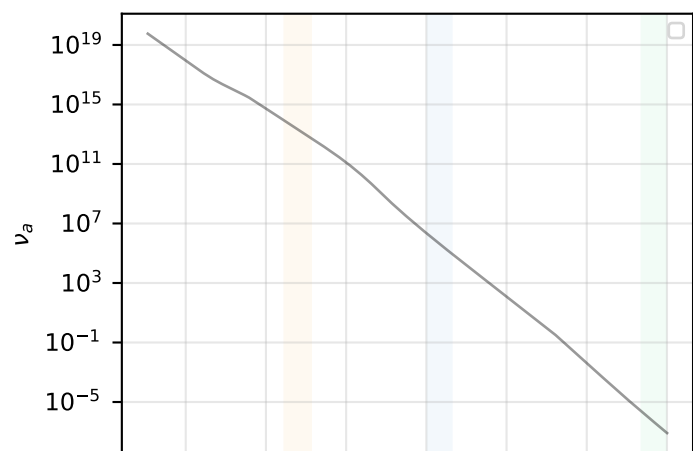
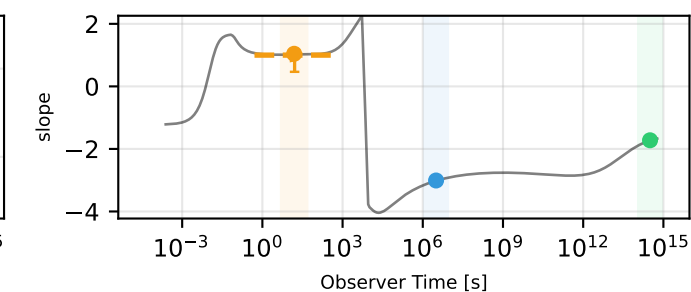
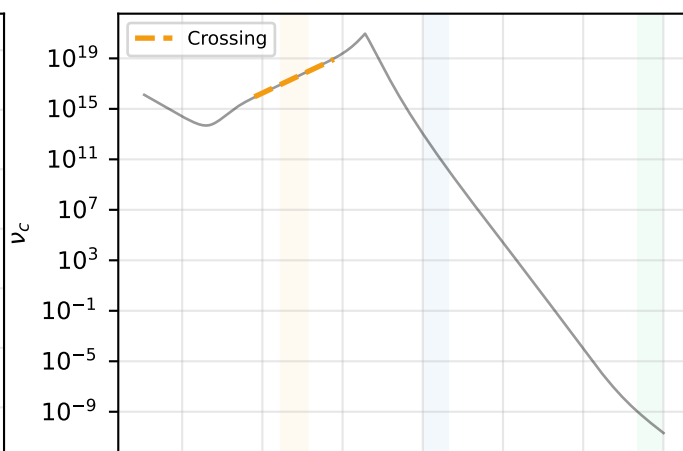
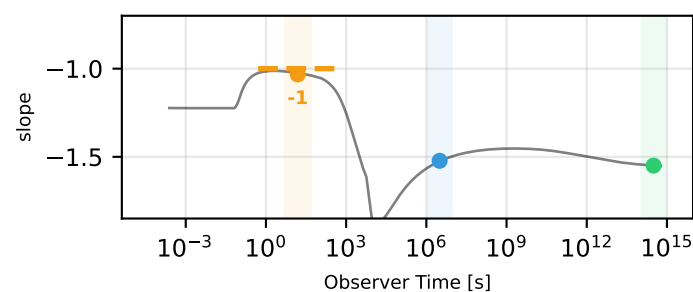
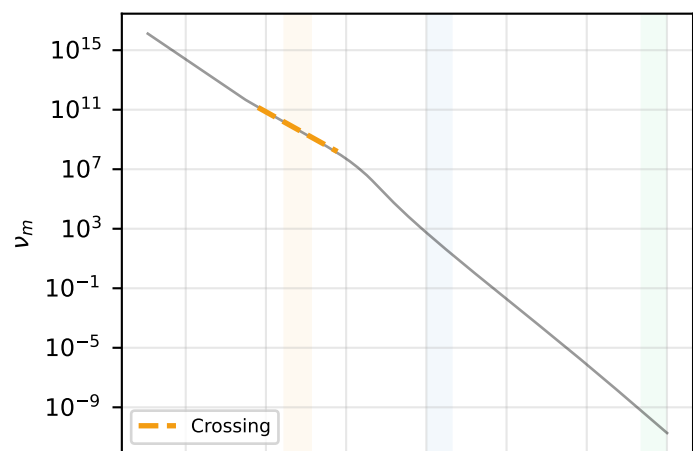
Forward Shock Frequencies: Wind



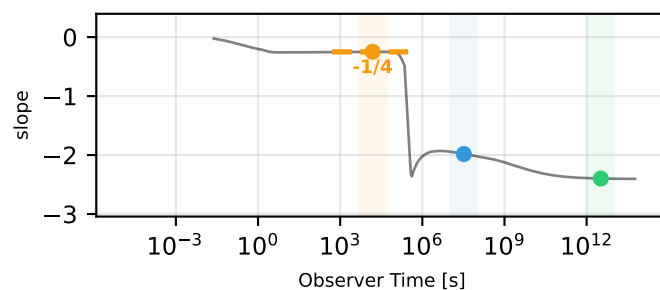
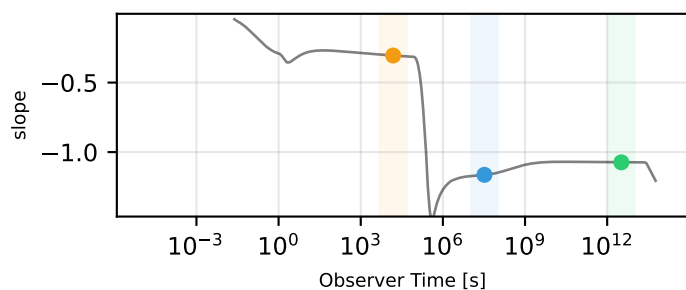
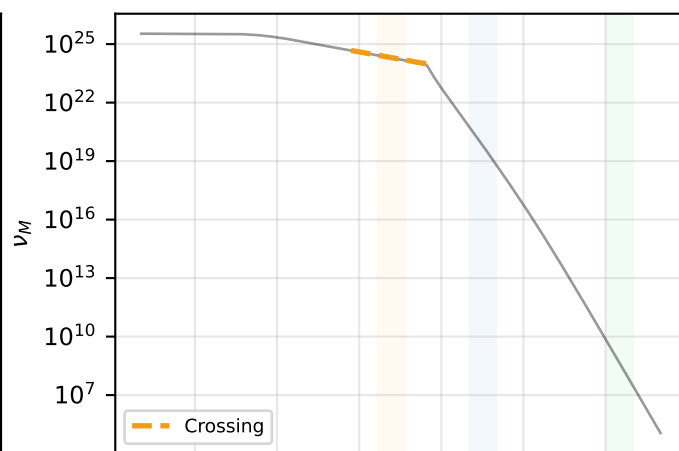
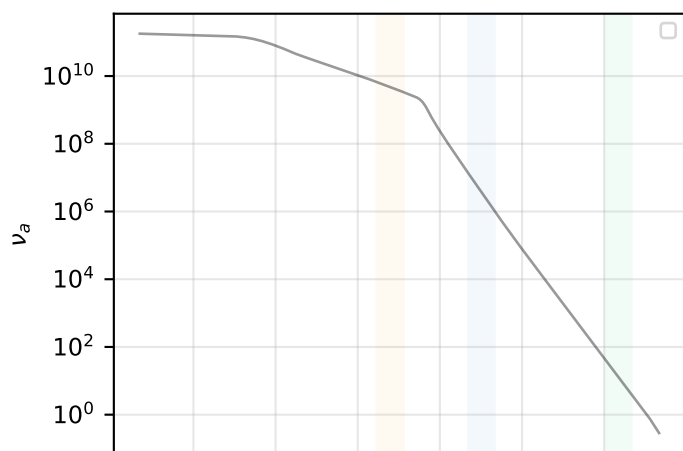
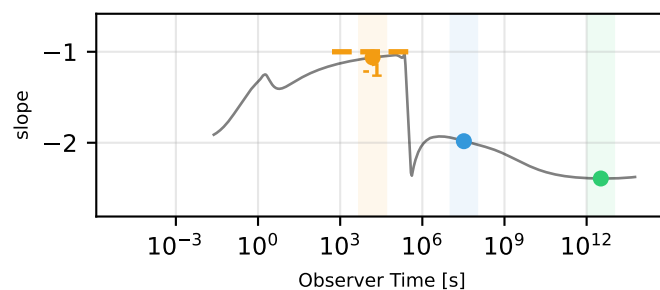
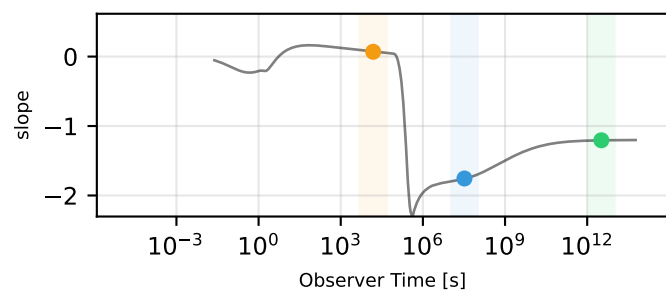
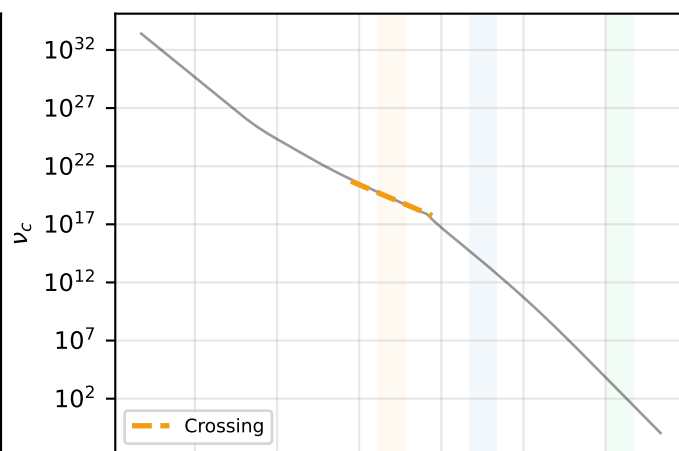
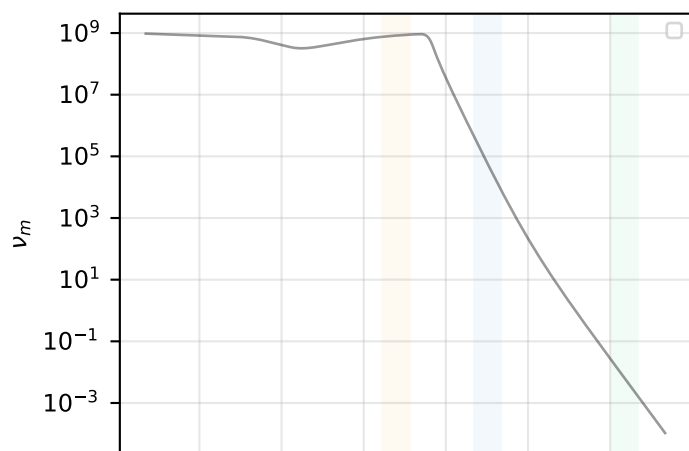
Reverse Shock Frequencies — Thin Shell: ISM



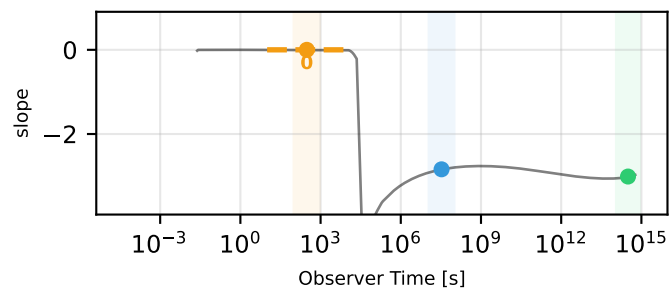
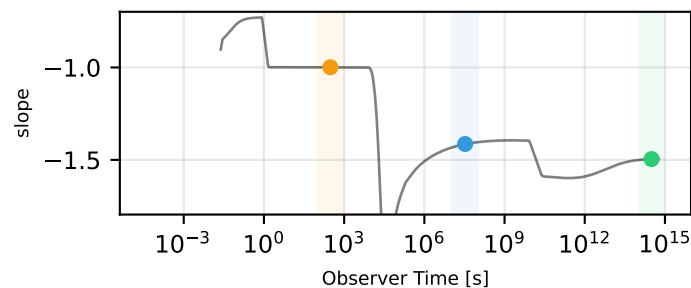
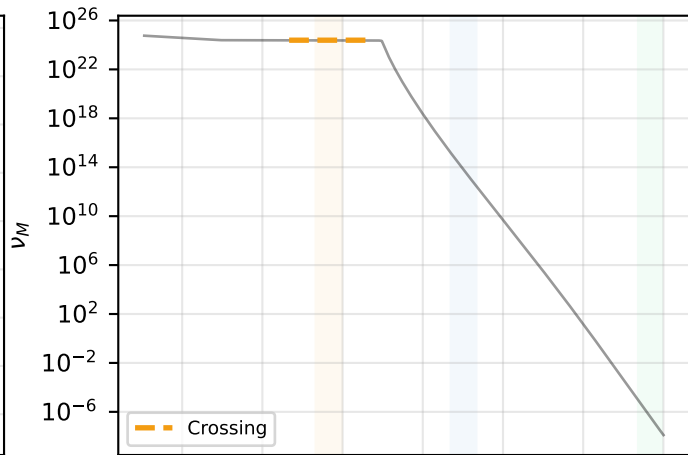
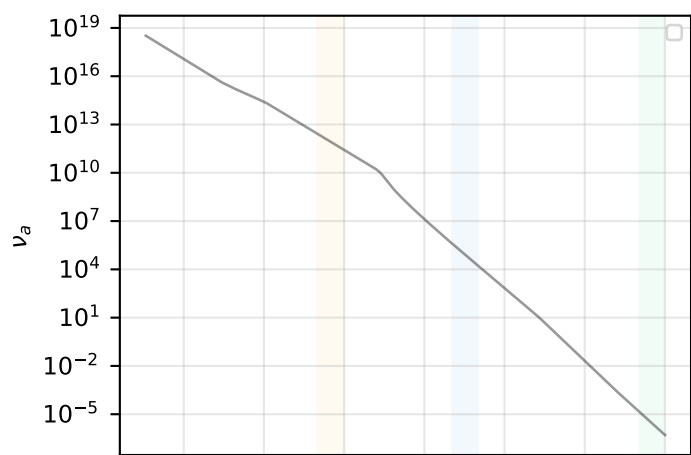
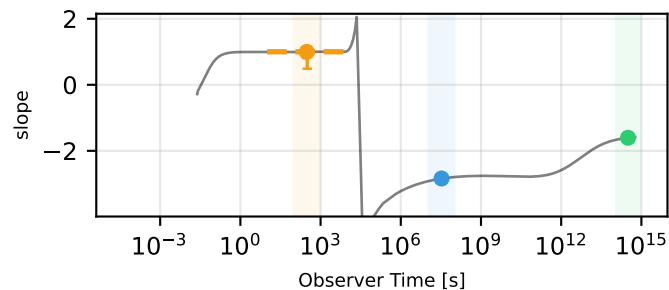
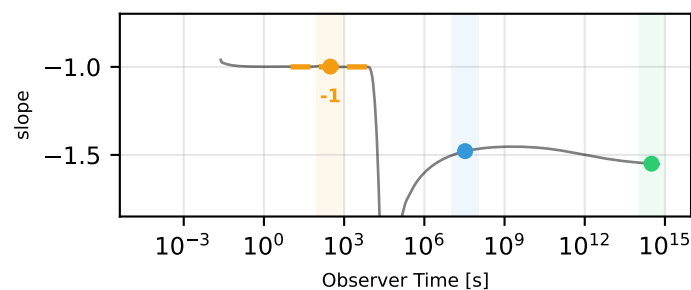
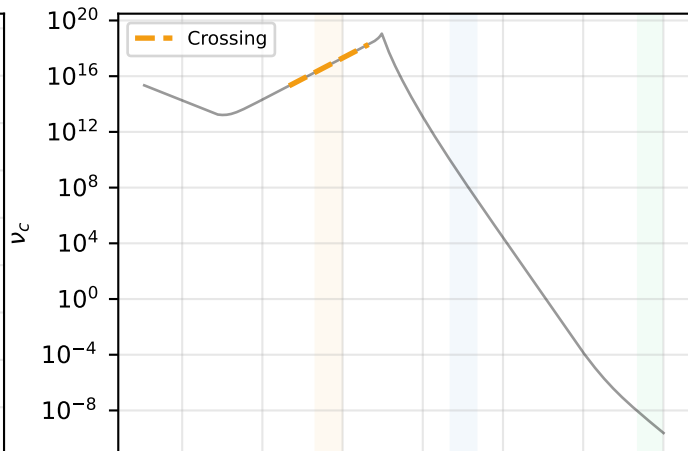
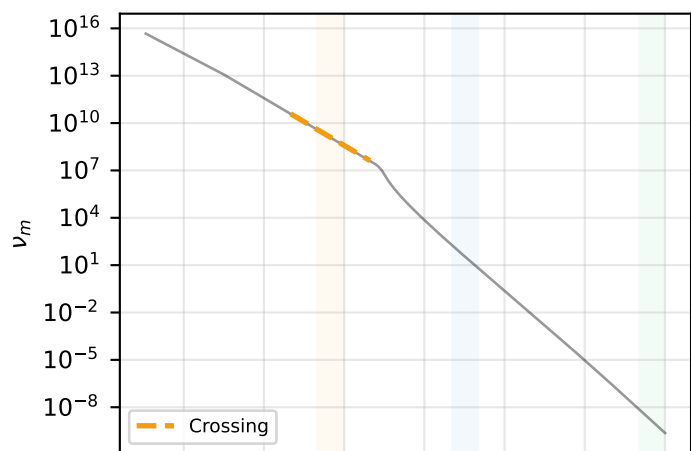
Reverse Shock Frequencies — Thin Shell: Wind



Reverse Shock Frequencies — Thick Shell: ISM



Reverse Shock Frequencies — Thick Shell: Wind



Section 2

Benchmark Results

Performance timing and resolution convergence analysis

Benchmark Report Guide

This document describes the benchmark validation framework for VegasAfterglow, which assesses numerical convergence and computational performance across physical configurations.

1. Configuration Space

The benchmark suite systematically tests a grid of physical scenarios and numerical settings to characterize code behavior across the parameter space relevant for GRB afterglow modeling.

1.1 Physical Parameters

Parameter	Options	Description
Jet Structure	tophat, gaussian, powerlaw, two_component	Angular energy profile
External Medium	ISM, Wind	Density profile: constant (ISM) or $\propto r^{-2}$ (Wind)
Radiation	synchrotron, full_ssc, fast_cooling, steep/flat_spectrum, rvs_sync_thin, rvs_sync_thick	Radiation physics
Viewing Angle	$\theta_v/\theta_c = 0, 2, 4$	On-axis (0) vs off-axis (>1)

1.2 Numerical Resolution

Resolution controls the discretization density in each computational dimension. The fiducial values represent the recommended default settings. Note that θ and t grids enforce a minimum total point count regardless of the ppd value, so low ppd settings may not reduce the actual grid size.

Dimension	Symbol	Unit	Fiducial	Test Range
Azimuthal angle	φ	per degree	0.1	0.1 - 0.25
Polar angle	θ	per degree	0.25	0.25 - 2.0
Observer time	t	per decade	10	10 - 25

1.3 Frequency Bands

Convergence is evaluated independently at three representative frequencies spanning the electromagnetic spectrum.

Band	Frequency (Hz)
Radio	10^9

Band	Frequency (Hz)
Optical	4.84×10^{14}
X-ray	10^{18}

2. Convergence Criteria

Numerical accuracy is quantified by comparing results at each resolution to a high-resolution reference run. Both mean and maximum relative errors across the light curve are evaluated.

Status	Criteria
PASS	mean error < 5% AND max error < 15%
ACCEPTABLE	mean error < 5% AND max error >= 15%
FAIL	mean error >= 5%

3. Summary Grid

The summary grid provides a compact overview of convergence status for all tested configurations on a single page.

3.1 Layout

Each cell represents one model configuration (jet, medium, viewing angle). Cells are arranged to facilitate comparison across jet types and viewing angles.

3.2 Cell Contents

Line	Content
1	Model ID
2	Configuration shorthand (jet/medium/angle_ratio)
3	Maximum error at fiducial resolution

3.3 Color Coding

Color	Status
Green	PASS
Blue	ACCEPTABLE
Pink	FAIL

Color	Status
Gray	No data

4. Overview Plots

The overview page provides performance profiling across configurations, helping identify computational bottlenecks and compare execution times.

4.1 Panel Layout

Position	Content
Top-left	Light curve computation time by jet type
Top-right	Stage breakdown (profiling build) or resolution cost scaling
Bottom-left	Medium comparison (ISM vs Wind)
Bottom-right	Wind/ISM speed ratio

4.2 Timing Metric

Each configuration is timed by computing a 30-point broadband light curve ($t = 10^2$ to 10^8 s) at the fiducial resolution. The reported time includes dynamics computation and flux evaluation in a single `flux_density` call.

4.3 Stage Breakdown

When built with profiling enabled (`pip install -e ".[test]" --config-settings=cmake.define.AFTERGLOW_PROFILE=ON`), the top-right panel shows a stacked bar chart of per-stage CPU cost for each jet/medium combination. The stages correspond to the internal C++ computation pipeline:

Stage	Description
mesh	Coordinate grid generation
shock_dynamics	Forward/reverse shock ODE integration
EAT_grid	Equal arrival time surface grid
syn_electrons	Synchrotron electron distribution
syn_photons	Synchrotron photon spectrum
cooling	SSC/IC cooling corrections
sync_flux	Synchrotron flux integration
ic_photons	Inverse Compton photon spectrum

Stage	Description
ssc_flux	SSC flux integration

Without profiling, the panel falls back to showing total resolution cost scaling.

5. Per-Model Convergence Pages

Each configuration receives a detailed convergence analysis page showing how accuracy and performance vary with resolution.

5.1 Row Contents

The page displays a 4x3 grid where each column corresponds to one resolution dimension (ϕ , θ , t) and each row shows a different metric.

Row	Y-axis	Threshold
1	Maximum relative error	15%
2	Mean relative error	5%
3	CPU time (ms)	-
4	Flux (mJy)	-

5.2 Plot Features

Feature	Meaning
Star marker	Fiducial resolution
Dashed line	Error threshold
Solid curves	Resolution \geq fiducial
Dotted curves	Resolution $<$ fiducial

5.3 Status Indicator

The page header displays convergence status with color coding matching Section 3.3.

6. Interpreting Results

6.1 Light Curve Convergence

The bottom row plots all tested resolutions together on the same axes. Visual spread between curves indicates resolution dependence.

Pattern	Interpretation
No spread (curves overlap)	Converged
Spread in dashed lines only	Not converged below fiducial, acceptable at fiducial
Spread in solid lines	Not converged even above fiducial resolution

6.2 Error Convergence

The top two rows show how errors decrease as resolution increases. The shape of these curves indicates convergence quality.

Pattern	Interpretation
Monotonic decrease	Stable convergence
Plateau	Noise floor or discretization limit
Non-monotonic	Potential numerical instability

6.3 Performance Scaling

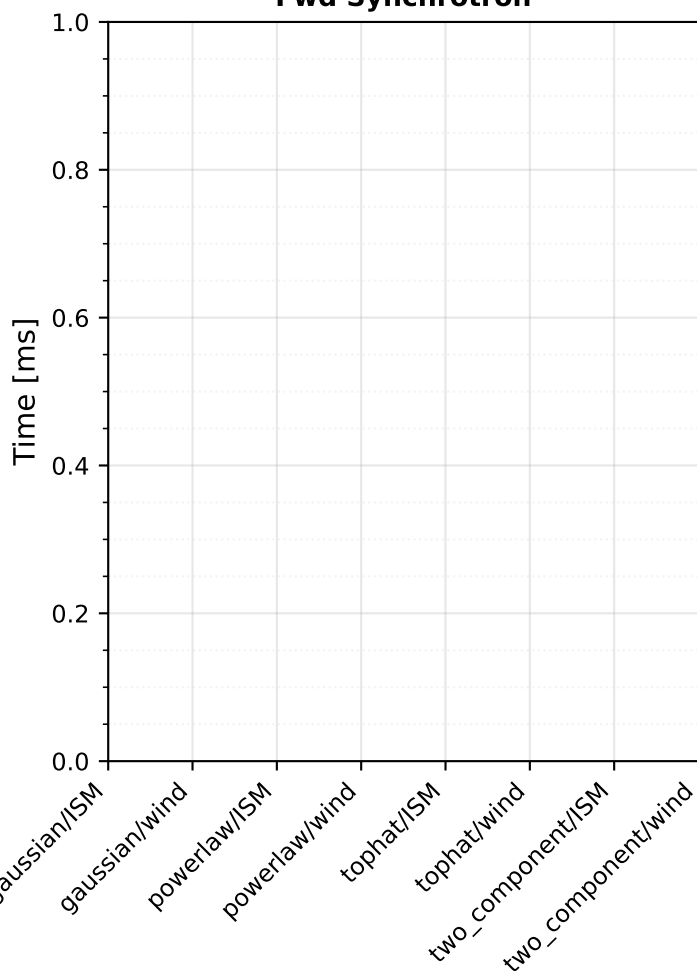
Computational cost typically scales as:

- Linear with time resolution (t_{pd})
- Quadratic with angular resolution ($\phi_{pd} \times \theta_{pd}$)

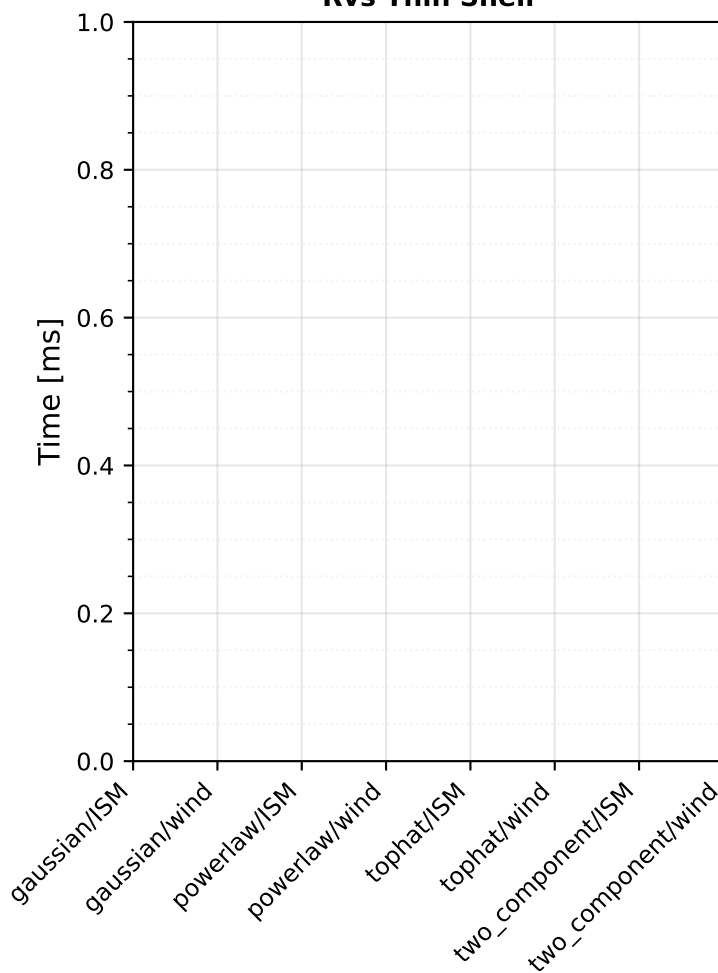
Wind medium simulations generally require more computation due to the radially-varying density profile. However, the medium-aware adaptive grid often produces smaller grids for wind (earlier deceleration time), which can offset this cost.

Benchmark Overview (On-axis, $\theta_v=0$)

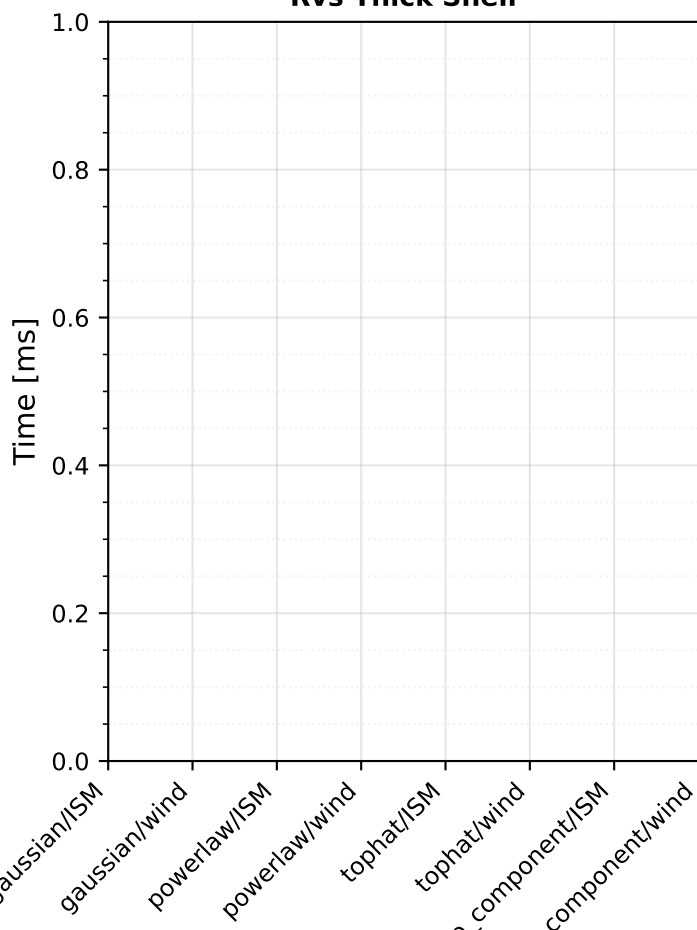
Fwd Synchrotron



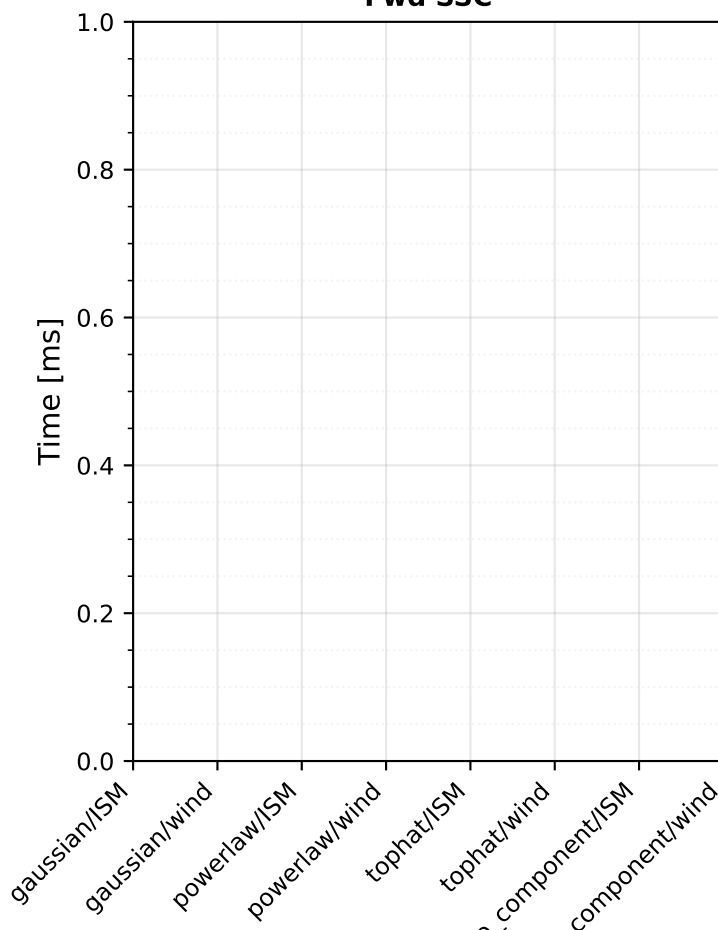
Rvs Thin Shell



Rvs Thick Shell

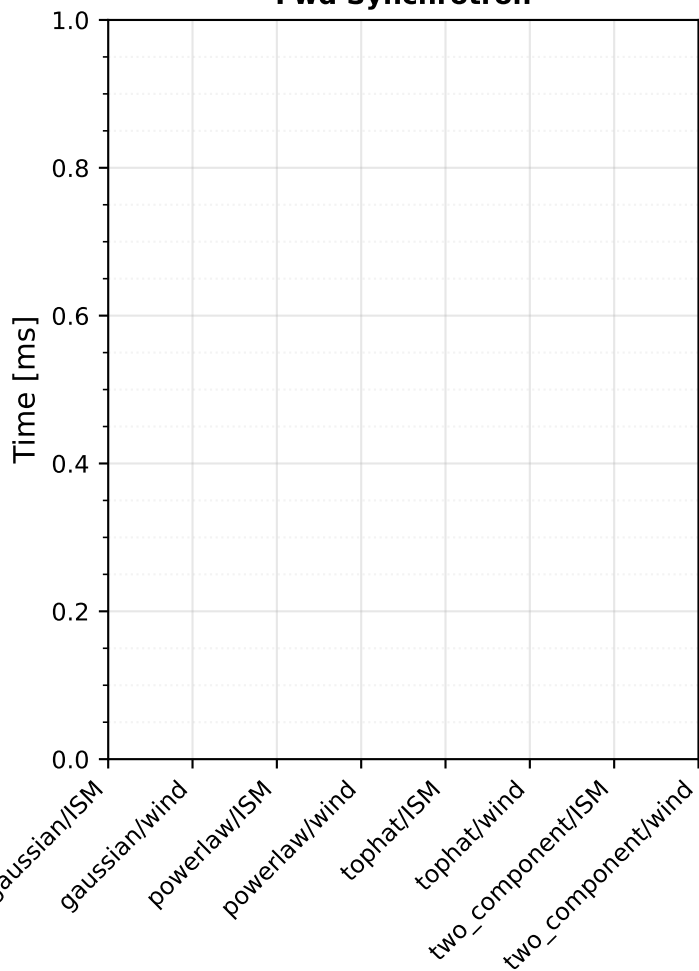


Fwd SSC

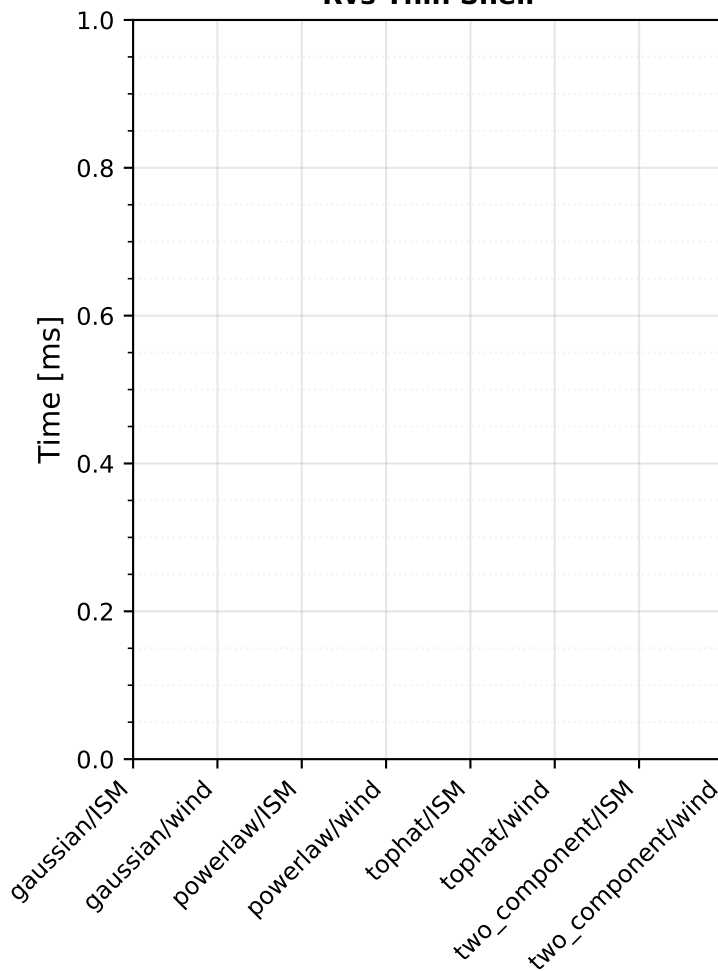


Benchmark Overview (Off-axis, $\theta_v/\theta_c > 1$)

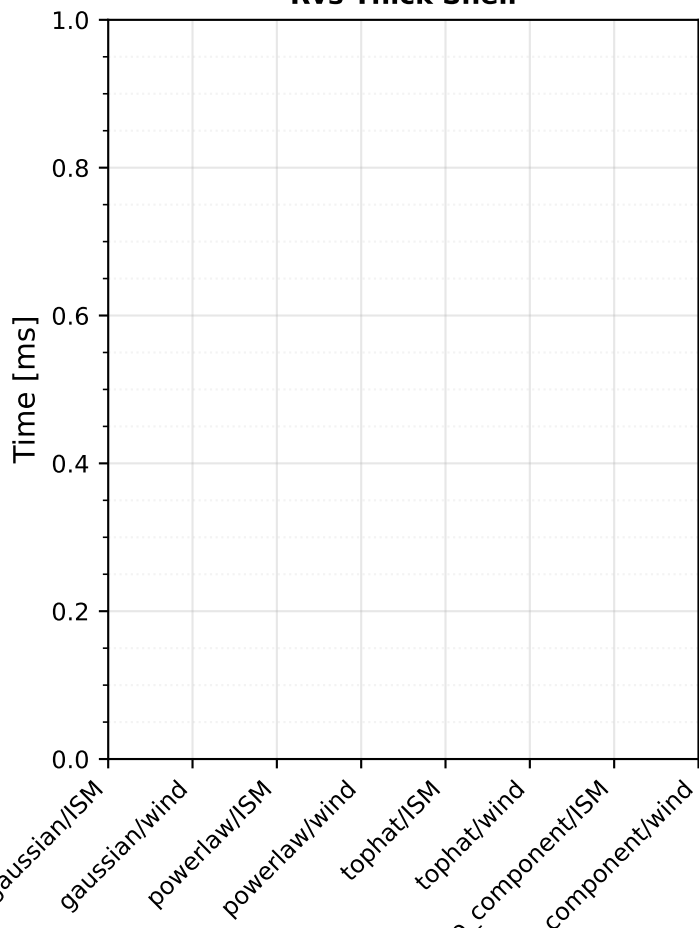
Fwd Synchrotron



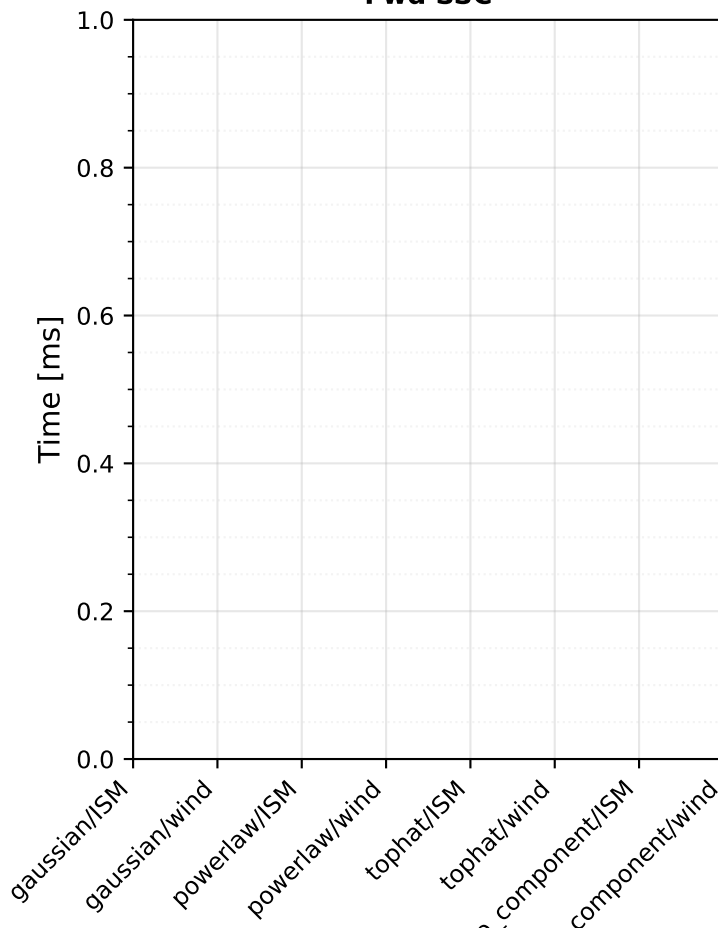
Rvs Thin Shell



Rvs Thick Shell



Fwd SSC



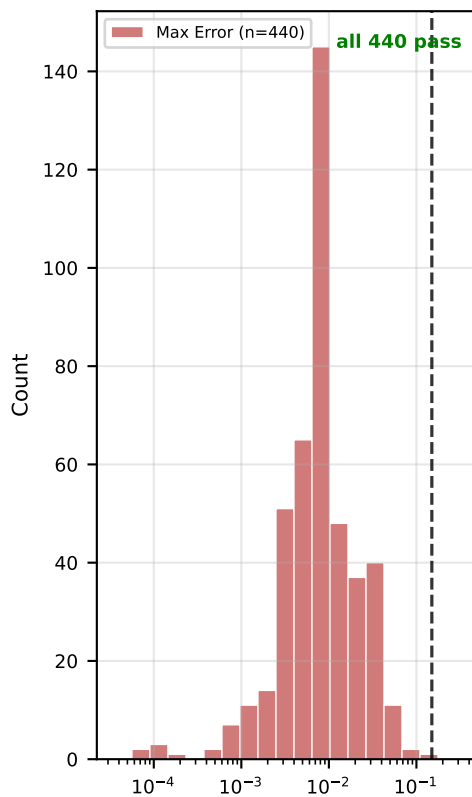
Resolution Convergence Summary

Pass: 160 | Acceptable: 0 | Fail: 0 | No Data: 0

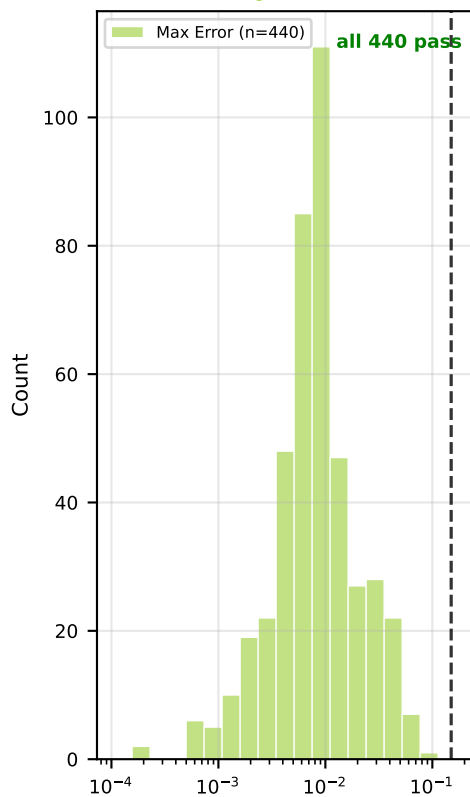
#1 topha/ISM/θ0 synchrotron ε=1.1e-02	#2 topha/ISM/θ1 synchrotron ε=3.9e-02	#3 topha/ISM/θ2 synchrotron ε=5.6e-03	#4 topha/ISM/θ4 synchrotron ε=5.0e-03	#5 topha/ISM/θ0 full_ssc ε=4.9e-02	#6 topha/ISM/θ1 full_ssc ε=5.2e-02	#7 topha/ISM/θ2 full_ssc ε=1.1e-02	#8 topha/ISM/θ4 full_ssc ε=9.8e-03	#9 topha/ISM/θ0 ssc_kn ε=4.9e-02	#10 topha/ISM/θ1 ssc_kn ε=5.2e-02
#11 topha/ISM/θ2 ssc_kn ε=1.0e-02	#12 topha/ISM/θ4 ssc_kn ε=6.9e-03	#13 topha/ISM/θ0 rvs_sync_thin ε=4.6e-02	#14 topha/ISM/θ1 rvs_sync_thin ε=9.5e-02	#15 topha/ISM/θ2 rvs_sync_thin ε=5.7e-02	#16 topha/ISM/θ4 rvs_sync_thin ε=6.3e-02	#17 topha/ISM/θ0 rvs_sync_thick ε=2.9e-02	#18 topha/ISM/θ1 rvs_sync_thick ε=3.2e-02	#19 topha/ISM/θ2 rvs_sync_thick ε=3.0e-02	#20 topha/ISM/θ4 rvs_sync_thick ε=3.0e-02
#21 topha/win/θ0 synchrotron ε=8.1e-03	#22 topha/win/θ1 synchrotron ε=3.1e-02	#23 topha/win/θ2 synchrotron ε=5.5e-03	#24 topha/win/θ4 synchrotron ε=1.1e-02	#25 topha/win/θ0 full_ssc ε=1.7e-02	#26 topha/win/θ1 full_ssc ε=3.0e-02	#27 topha/win/θ2 full_ssc ε=2.0e-02	#28 topha/win/θ4 full_ssc ε=1.4e-01	#29 topha/win/θ0 ssc_kn ε=1.5e-02	#30 topha/win/θ1 ssc_kn ε=3.1e-02
#31 topha/win/θ2 ssc_kn ε=1.3e-02	#32 topha/win/θ4 ssc_kn ε=1.9e-02	#33 topha/win/θ0 rvs_sync_thin ε=2.1e-02	#34 topha/win/θ1 rvs_sync_thin ε=6.5e-02	#35 topha/win/θ2 rvs_sync_thin ε=8.6e-02	#36 topha/win/θ4 rvs_sync_thin ε=5.4e-02	#37 topha/win/θ0 rvs_sync_thick ε=2.8e-02	#38 topha/win/θ1 rvs_sync_thick ε=3.5e-02	#39 topha/win/θ2 rvs_sync_thick ε=2.9e-02	#40 topha/win/θ4 rvs_sync_thick ε=2.9e-02
#41 gauss/ISM/θ0 synchrotron ε=1.7e-02	#42 gauss/ISM/θ1 synchrotron ε=1.1e-02	#43 gauss/ISM/θ2 synchrotron ε=9.7e-03	#44 gauss/ISM/θ4 synchrotron ε=6.9e-03	#45 gauss/ISM/θ0 full_ssc ε=2.9e-02	#46 gauss/ISM/θ1 full_ssc ε=3.7e-02	#47 gauss/ISM/θ2 full_ssc ε=1.2e-02	#48 gauss/ISM/θ4 full_ssc ε=1.1e-02	#49 gauss/ISM/θ0 ssc_kn ε=2.9e-02	#50 gauss/ISM/θ1 ssc_kn ε=3.7e-02
#51 gauss/ISM/θ2 ssc_kn ε=1.2e-02	#52 gauss/ISM/θ4 ssc_kn ε=9.6e-03	#53 gauss/ISM/θ0 rvs_sync_thin ε=3.5e-02	#54 gauss/ISM/θ1 rvs_sync_thin ε=2.1e-02	#55 gauss/ISM/θ2 rvs_sync_thin ε=3.9e-02	#56 gauss/ISM/θ4 rvs_sync_thin ε=2.5e-02	#57 gauss/ISM/θ0 rvs_sync_thick ε=4.4e-02	#58 gauss/ISM/θ1 rvs_sync_thick ε=3.9e-02	#59 gauss/ISM/θ2 rvs_sync_thick ε=4.0e-02	#60 gauss/ISM/θ4 rvs_sync_thick ε=4.0e-02
#61 gauss/win/θ0 synchrotron ε=1.3e-02	#62 gauss/win/θ1 synchrotron ε=9.5e-03	#63 gauss/win/θ2 synchrotron ε=9.6e-03	#64 gauss/win/θ4 synchrotron ε=9.4e-03	#65 gauss/win/θ0 full_ssc ε=1.1e-02	#66 gauss/win/θ1 full_ssc ε=1.0e-02	#67 gauss/win/θ2 full_ssc ε=1.0e-02	#68 gauss/win/θ4 full_ssc ε=1.9e-02	#69 gauss/win/θ0 ssc_kn ε=1.2e-02	#70 gauss/win/θ1 ssc_kn ε=1.0e-02
#71 gauss/win/θ2 ssc_kn ε=1.0e-02	#72 gauss/win/θ4 ssc_kn ε=1.9e-02	#73 gauss/win/θ0 rvs_sync_thin ε=4.1e-02	#74 gauss/win/θ1 rvs_sync_thin ε=4.0e-02	#75 gauss/win/θ2 rvs_sync_thin ε=1.6e-02	#76 gauss/win/θ4 rvs_sync_thin ε=1.9e-02	#77 gauss/win/θ0 rvs_sync_thick ε=6.3e-02	#78 gauss/win/θ1 rvs_sync_thick ε=7.7e-02	#79 gauss/win/θ2 rvs_sync_thick ε=5.4e-02	#80 gauss/win/θ4 rvs_sync_thick ε=5.3e-02
#81 power/ISM/θ0 synchrotron ε=2.5e-02	#82 power/ISM/θ1 synchrotron ε=1.6e-02	#83 power/ISM/θ2 synchrotron ε=1.2e-02	#84 power/ISM/θ4 synchrotron ε=1.1e-02	#85 power/ISM/θ0 full_ssc ε=2.7e-02	#86 power/ISM/θ1 full_ssc ε=5.8e-02	#87 power/ISM/θ2 full_ssc ε=1.2e-02	#88 power/ISM/θ4 full_ssc ε=1.4e-02	#89 power/ISM/θ0 ssc_kn ε=2.7e-02	#90 power/ISM/θ1 ssc_kn ε=5.8e-02
#91 power/ISM/θ2 ssc_kn ε=2.0e-02	#92 power/ISM/θ4 ssc_kn ε=1.3e-02	#93 power/ISM/θ0 rvs_sync_thin ε=4.9e-02	#94 power/ISM/θ1 rvs_sync_thin ε=1.9e-02	#95 power/ISM/θ2 rvs_sync_thin ε=2.1e-02	#96 power/ISM/θ4 rvs_sync_thin ε=1.1e-02	#97 power/ISM/θ0 rvs_sync_thick ε=3.4e-02	#98 power/ISM/θ1 rvs_sync_thick ε=3.0e-02	#99 power/ISM/θ2 rvs_sync_thick ε=3.0e-02	#100 power/ISM/θ4 rvs_sync_thick ε=3.0e-02
#101 power/win/θ0 synchrotron ε=1.8e-02	#102 power/win/θ1 synchrotron ε=1.3e-02	#103 power/win/θ2 synchrotron ε=1.1e-02	#104 power/win/θ4 synchrotron ε=8.3e-03	#105 power/win/θ0 full_ssc ε=1.6e-02	#106 power/win/θ1 full_ssc ε=1.3e-02	#107 power/win/θ2 full_ssc ε=1.1e-02	#108 power/win/θ4 full_ssc ε=1.2e-02	#109 power/win/θ0 ssc_kn ε=1.7e-02	#110 power/win/θ1 ssc_kn ε=1.3e-02
#111 power/win/θ2 ssc_kn ε=1.1e-02	#112 power/win/θ4 ssc_kn ε=1.3e-02	#113 power/win/θ0 rvs_sync_thin ε=5.3e-02	#114 power/win/θ1 rvs_sync_thin ε=3.8e-02	#115 power/win/θ2 rvs_sync_thin ε=1.4e-02	#116 power/win/θ4 rvs_sync_thin ε=1.2e-02	#117 power/win/θ0 rvs_sync_thick ε=4.7e-02	#118 power/win/θ1 rvs_sync_thick ε=5.7e-02	#119 power/win/θ2 rvs_sync_thick ε=6.0e-02	#120 power/win/θ4 rvs_sync_thick ε=6.0e-02
#121 two_c/ISM/θ0 synchrotron ε=1.1e-02	#122 two_c/ISM/θ1 synchrotron ε=4.8e-02	#123 two_c/ISM/θ2 synchrotron ε=4.4e-02	#124 two_c/ISM/θ4 synchrotron ε=1.3e-02	#125 two_c/ISM/θ0 full_ssc ε=2.1e-02	#126 two_c/ISM/θ1 full_ssc ε=5.2e-02	#127 two_c/ISM/θ2 full_ssc ε=4.4e-02	#128 two_c/ISM/θ4 full_ssc ε=2.4e-02	#129 two_c/ISM/θ0 ssc_kn ε=2.8e-02	#130 two_c/ISM/θ1 ssc_kn ε=5.2e-02
#131 two_c/ISM/θ2 ssc_kn ε=4.4e-02	#132 two_c/ISM/θ4 ssc_kn ε=2.7e-02	#133 two_c/ISM/θ0 rvs_sync_thin ε=4.1e-02	#134 two_c/ISM/θ1 rvs_sync_thin ε=5.0e-02	#135 two_c/ISM/θ2 rvs_sync_thin ε=4.0e-02	#136 two_c/ISM/θ4 rvs_sync_thin ε=3.8e-02	#137 two_c/ISM/θ0 rvs_sync_thick ε=3.0e-02	#138 two_c/ISM/θ1 rvs_sync_thick ε=3.1e-02	#139 two_c/ISM/θ2 rvs_sync_thick ε=3.5e-02	#140 two_c/ISM/θ4 rvs_sync_thick ε=3.0e-02
#141 two_c/win/θ0 synchrotron ε=1.1e-02	#142 two_c/win/θ1 synchrotron ε=1.8e-02	#143 two_c/win/θ2 synchrotron ε=1.8e-02	#144 two_c/win/θ4 synchrotron ε=8.0e-03	#145 two_c/win/θ0 full_ssc ε=1.3e-02	#146 two_c/win/θ1 full_ssc ε=1.4e-02	#147 two_c/win/θ2 full_ssc ε=1.9e-02	#148 two_c/win/θ4 full_ssc ε=1.7e-02	#149 two_c/win/θ0 ssc_kn ε=1.5e-02	#150 two_c/win/θ1 ssc_kn ε=1.4e-02
#151 two_c/win/θ2 ssc_kn ε=2.1e-02	#152 two_c/win/θ4 ssc_kn ε=1.8e-02	#153 two_c/win/θ0 rvs_sync_thin ε=4.0e-02	#154 two_c/win/θ1 rvs_sync_thin ε=4.3e-02	#155 two_c/win/θ2 rvs_sync_thin ε=2.6e-02	#156 two_c/win/θ4 rvs_sync_thin ε=8.8e-02	#157 two_c/win/θ0 rvs_sync_thick ε=2.7e-02	#158 two_c/win/θ1 rvs_sync_thick ε=2.7e-02	#159 two_c/win/θ2 rvs_sync_thick ε=3.1e-02	#160 two_c/win/θ4 rvs_sync_thick ε=3.1e-02

Error Distribution Across All Configurations

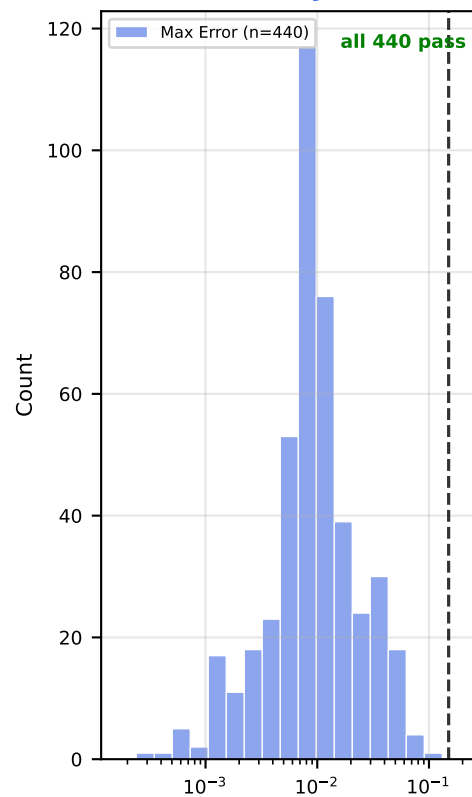
Radio



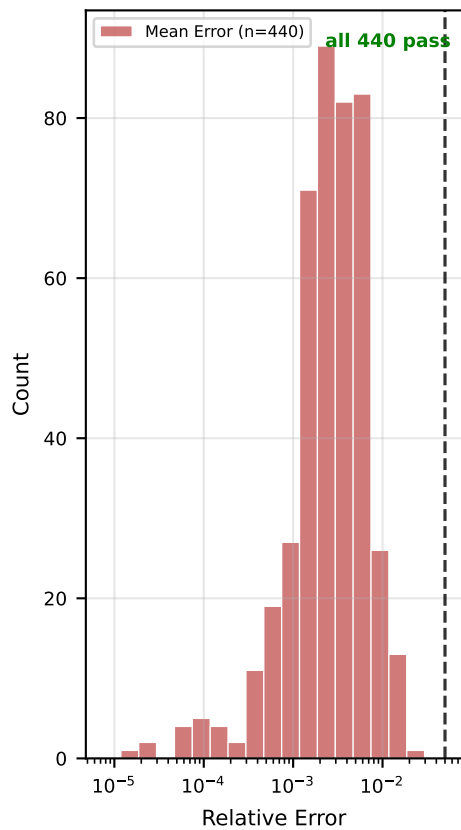
Optical



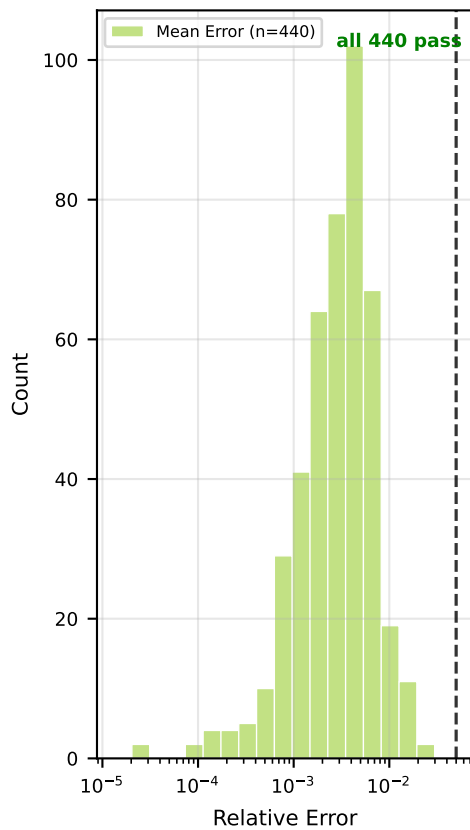
X-ray



Radio



Optical



X-ray

